2. Schumacher R, Seaver LH, Spranger J (2004) Introduction. In: Schumacher R, Seaver LH, Spranger J (eds) Fetal radiology, a diagnostic atlas, 1st edn. Springer, Berlin, pp 1–2
3. Ruano R, Molho M, Roume J et al (2004) Prenatal diagnosis of fetal skeletal dysplasias by combining two-dimensional and three-dimensional ultrasound and intrauterine three-dimensional helical computer tomography. Ultrasound Obstet Gynecol 24:134–140
4. Suzumura H, Kohno T, Nishimura G et al (2002) Prenatal diagnosis of hypochondrogenesis using fetal MRI: a case report. Pediatr Radiol 35:373–375
5. Garjian KV, Pretorius DH, Budorick NE et al (2000) Fetal skeletal dysplasia: three-dimensional US-initial experience. Radiology 21: 717–723
6. Cassart M, Massez A, Cos T et al (2007) Contribution of three dimensional computed tomography in the assessment of fetal skeletal dysplasia. Ultrasound Obstet Gynecol 29:537–543
7. Cassart M (2010) Suspected fetal skeletal malformations or bone diseases: how to explore. Pediatr Radiol 40:1046–1051
8. Boulet S, Althuser M, Nugues F et al (2009) Prenatal diagnosis of achondroplasia: new specific signs. Prenat Diagn 29:697–702
9. Victoria T, Epelman M, Coleman BG et al (2013) Low-dose fetal CT in the prenatal evaluation of skeletal dysplasia and other severe skeletal abnormalities. AJR Am J Roentgenol 200:989–1000
10. Miyazaki O, Nishimura G, Sago H et al (2012) Prenatal diagnosis of fetal skeletal dysplasia with 3D CT. Pediatr Radiol 42:842–852
11. Macé G, Sonigo P, Cormier-Daire V et al (2013) Three-dimensional helical computed tomography in prenatal diagnosis of fetal skeletal dysplasia. Ultrasound Obstet Gynecol 42:161–168
12. Guillerman RP (2011) Newer CT applications and their alternatives: what is appropriate in children? Pediatr Radiol 41:s534–s548
13. The American College of Obstetrics and Gynecologists (2004) Guidelines for diagnostic imaging pregnancy. AOCG committee opinion No. 299. 104:647–651
14. Slovis TL, Hall ET, Huda W et al (2002) ALARA conference executive summary. Pediatr Radiol 32:221
15. Frush DP (2011) Justification and optimization of CT in children: how are we performing? Pediatr Radiol 41:s467–s471
16. Bach-Segura P (2006) Etude du squelette fœtal en scanner multibarrette: optimisation du protocole, traitement de l'image. J Radiol 87:1358
17. IAEA Radiation Protection of Patients (RPOP). Diagnostic reference levels (DRLs) in CT. https://rpop.iaea.org/RPOP/RPoP/Content/InformationFor/HealthProfessionals/1_Radiology/ComputedTomography/diagnostic-reference-levels.htm
18. Institute of Physics and Engineering in Medicine (IPEM) (2004) Guidance on the establishment and use of diagnostic reference levels for medical X-ray examinations. IPEM report 88.
19. European Commissions. Radiation protection 109. Guidance on diagnostic reference levels (DRLs) for medical exposure. http://ec.europa.eu/energy/nuclear/radiation_protection/doc/publication/109_en.pdf#search='European+Commission+%28EC%29.+Radiation+protection+109.+Guidance+on+diagnostic+reference+levels+%28DRLs%29+for+medical+exposures'
20. ACR–AAPM practice guideline for diagnostic reference levels and achievable dose in medical X-ray imaging. Revised 2013 (Resolution 47). http://www.acr.org/~/media/796DE35AA407447DB81CEB5612B4553D.pdf#search='ACR+PRACTICE+GUIDELINE+FOR+DIAGNOSTIC+REFERENCE+LEVELS+IN+MEDICAL+XRAY+IMAGING%2C+Revised+2008++Resolution+3'
21. Thomas KE (2011) CT utilization—trends and developments beyond the United States' borders. Pediatr Radiol 41:s562–s566
22. Victoria T, Epelman M, Bebbington M et al (2012) Low-dose fetal CT for evaluation of severe congenital skeletal anomalies; preliminary experience. Pediatr Radiol 42:s142–s149
23. Shrimpton PC, Hillier MA, Lewis MA et al (2006) National survey of doses from CT in the UK: 2003. Br J Radiol 79:968–980
24. Kritsaneepaiboon S, Trinavarat P, Visrutarathna P (2012) Survey of pediatric MDCT radiation dose from university hospitals in Thailand: a preliminary for national dose survey. Acta Radiol 52:820–826
25. Watson DJ, Coakley KS (2010) Paediatric CT reference doses based on weight and CT dosimetry phantom size: local experience using a 64-slice CT scanner. Pediatr Radiol 40:693–703
26. Shoda S, Hamada H, Oki A et al (1997) Diagnosis of fetal anomalies by three-dimensional imaging using helical computed tomography. Prenat Diagn 17:670–674
27. Miyazaki O, Nishimura G, Sago H et al (2007) Prenatal diagnosis of chondrodysplasia punctata tibia-metacarpal type using multidetector CT and three-dimensional reconstruction. Pediatr Radiol 37:1151–1154
28. Tsutsumi S, Sawai H, Nishimura G et al (2008) Prenatal diagnosis of thanatophoric dysplasia by 3-D helical computed tomography and genetic analysis. Fetal Diagn Ther 24:420–424
29. Yamada T, Nishimura G, Nishida K et al (2011) Prenatal diagnosis of short-rib polydactyly syndrome type 3 (Verma-Naumoff type) by three-dimensional computed tomography. J Obstet Gynaecol Res 37:151–155
30. Bonnefoy O, Delbosc JM, Maugey-Laulom B et al (2006) Prenatal diagnosis of hypochondroplasia: three-dimensional multislice computed tomography findings and molecular analysis. Fetal Diagn Ther 21:18–21
31. Felmlee JP, Gray JE, Leetzow ML et al (1990) Estimated fetal radiation dose from multislice CT studies. AJR Am J Roentgenol 154:185–190
32. ICRP (2000) Annals of the ICRP publication 84, 30(1). Elsevier Science Ltd, London
33. Hurwitz LM, Yoshizumi T, Reiman RE et al (2005) Radiation dose to the fetus from body MDCT during early gestation. AJR Am J Roentgenol 186:871–876
34. Miyazaki O, Horiuchi T, Akahane M et al (2009) Radiation doses of three-dimensional MDCT for skeletal dysplasia: is the procedure warranted? Pediatr Radiol 39:S288–S327
35. Pearce MS, Salotti JA, Little MP et al (2012) Radiation exposure from CT scans in childhood and subsequent risk of leukemia and brain tumors: a retrospective cohort study. Lancet 380:499–505
36. http://www.gehealthcare.com/dose/how-we-can-help/computed-tomography.html. Accessed 19 Jan 2013

doi:10.1038/nature13750

DISEASE MODELS

Statins give bone growth a boost

The development of stem-cell-based models of two diseases that cause dwarfism reveals that statins — drugs that are used to treat high levels of blood cholesterol — may also promote cartilage formation and bone growth.

BJORN R. OLSEN

Many medical conditions can cause short stature, but a faulty gene encoding the protein FGFR3 is responsible for two-thirds of all forms of dwarfism in humans. FGFR3 normally controls a brake signal in the molecular machinery that regulates the growth of limb bones during childhood and adolescence. In 1 in every 10,000–30,000 births, genetic mutations cause FGFR3 to become overactive and so brake too hard. Although our understanding of the cellular processes that go awry in dwarfism is good, development of treatments has been hampered by a lack of efficient methods for screening and testing potential drugs. In a paper published on *Nature*'s website today, Yamashita *et al.*[1] report a major step forward in solving this problem, establishing a human-disease-based system for screening potential drugs to treat skeletal-growth defects.

In humans, the most common FGFR3 mutation results in achondroplasia, a disorder that causes short extremities, increased curvature of the spine and distortion of skull growth, resulting in substantial health problems[2]. More-severe mutations in FGFR3 can cause thanatophoric dysplasia, in which a small chest, and respiratory problems, may cause death either at or shortly after birth[3]. In both dysplasias, skeletal defects are caused by decreased proliferation and impaired maturation of cartilage-forming cells called chondrocytes within growing regions of bone[4]. It has not previously been possible to obtain chondrocytes from patients, but Yamashita and colleagues took advantage of improved cell-reprogramming techniques[5] to do just that.

The authors isolated skin cells from three individuals with thanatophoric dysplasia and converted the cells to induced pluripotent stem cells, which can give rise to any cell type in the body. Next, Yamashita and co-workers stimulated the stem cells to become chondrocytes, which had the same genetic make-up as the original patients. They then took advantage of the chondrocytes' ability to aggregate into cartilage-forming particles[6] to generate a system for analysing particles formed by thanatophoric dysplasia chondrocytes and by controls without the FGFR3 mutation. The authors compared the particles' similarities and differences as the different cells grew and matured over several weeks in culture (Fig. 1).

A major difference was that, compared to controls, thanatophoric dysplasia particles exhibited impaired maturation associated with degradation of cartilage. Remarkably, reducing FGFR3 levels or adding antibodies to block FGFR3 activity in dysplasia cultures restored growth and maturation of the cartilage-forming particles to normal levels. Yamashita and co-workers used their culture system to assay several molecules that affect either the response of cells to FGFR3 signals or the formation of chondrocytes from stem cells, to determine which could promote cartilage development in dysplastic cells. Molecules that had positive effects included C-type natriuretic peptide (CNP) and several statins, including lovastatin and rosuvastatin.

CNP has a positive effect on bone formation and growth[4], and its overexpression in chondrocytes counteracts dwarfism in a mouse model of achondroplasia[7]. As a result, CNP has been pursued as a potential achondroplasia treatment, although it is not an ideal candidate. A major obstacle is that the peptide, which must be injected, is degraded within minutes of being administered. A more stable version is effective in mouse models of achondroplasia and is currently in clinical trials, but still requires daily injections[8]. In addition, the effects of CNP on the cardiovascular system and the central nervous system raise the possibility of undesirable side effects if the drug is used long-term in children.

Statins — cholesterol-lowering drugs that are available in tablet form — provide an interesting alternative. Their safety has been evaluated in children with inherited high cholesterol[9], and evidence[10] suggests that early statin treatment improves the chances of children with this condition reaching the age of 30 without having a heart attack. In addition to their cholesterol-related properties, the drugs stimulate production of chondrocyte

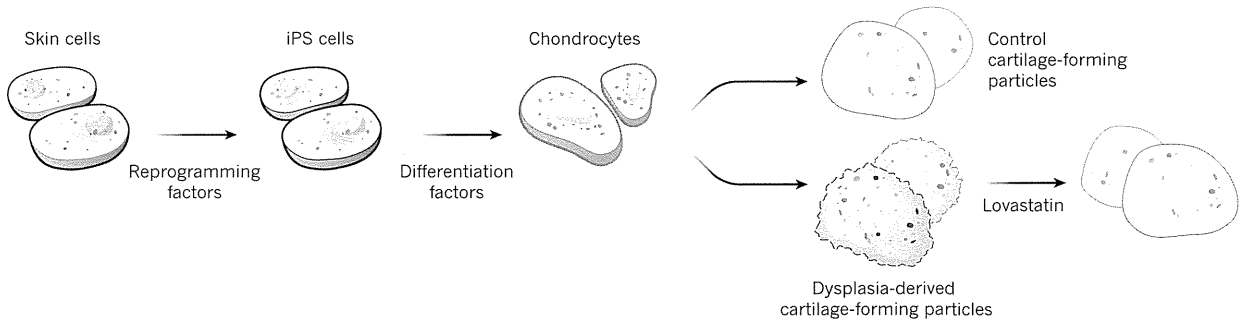

Figure 1 | A cell-based model of impaired bone growth. Yamashita *et al.*[1] isolated skin cells from people with thanatophoric dysplasia and from people with normal bone growth, and reprogrammed them to become induced pluripotent stem cells (iPS cells), which can give rise to every cell type of the body. They then added factors that caused the cells to differentiate into cartilage-forming cells called chondrocytes. Chondrocytes derived from controls produced normal cartilage-forming particles, but the particles formed from dysplasia-derived chondrocytes showed impaired growth and maturation. However, normal particle formation was restored when the drug lovastatin was added to the culture dish, highlighting a possible treatment for this disease.

molecules that make up the structure of cartilage[11], and repress production of cartilage-degrading enzymes[12]. In a series of compelling experiments, Yamashita *et al.* demonstrated that lovastatin stimulates production of cartilage components in thanatophoric dysplasia chondrocytes, and promotes the formation of chondrocytes from stem cells. It also restores cartilage formation by chondrocytes derived from people with achondroplasia. Finally, the authors showed that injecting rosuvastatin into mice with an achondroplasia-causing defect in FGFR3 partially restored bone growth in the limbs and head.

What are the mechanisms underlying these striking effects? Yamashita and colleagues' study does not provide the full answer. However, the authors do find that high levels of FGFR3 protein, but not messenger RNA, are reduced to normal levels when lovastatin is added to cultures of particles derived from people with either form of dysplasia. This suggests that statins stimulate degradation of FGFR3. Cellular protein-degradation machines called proteasomes might be involved, because adding a proteasome inhibitor to lovastatin-containing cultures increased levels of FGFR3. The researchers speculate that this is related to the ability of statins to lower cholesterol in cells, and to destabilize cell membranes so that FGFR3 (which spans the membrane) is more easily internalized and degraded, but this remains to be determined.

If the ability of statins to restore cartilage-particle growth is found to be independent of their cholesterol-lowering properties, it may be possible to modify the drugs such that these two effects are separated. However, if the cartilage-promoting effect of statins is a direct consequence of a decrease in cholesterol, extreme care is needed before using the drugs to treat children with achondroplasia. It will be crucial to ensure that cholesterol levels in these children are maintained at reasonable levels.

Between the ages of 25 and 35, mortality related to heart disease is more than 10 times higher in people with achondroplasia than in the general population[13,14]. The reasons for this are not understood, and limited data suggest that serum cholesterol levels in children with achondroplasia are in the high normal range[15]. Whether statin treatment would help to reduce this mortality is therefore unclear.

In summary, Yamashita *et al.* have established a disease model of achondroplasia and related dysplasias based on pluripotent stem cells. The results of the study raise the possibility that statins might be effective in treating children with these disorders. Furthermore, the authors' system allows screening of additional compounds in the search for even safer drugs. ■

Bjorn R. Olsen *is in the Department of Cell Biology, Harvard Medical School, Boston, Massachusetts 02115, USA.*
e-mail: bjorn_olsen@hms.harvard.edu

1. Yamashita, A. *et al. Nature* http://dx.doi.org/10.1038/nature13775 (2014).
2. Shiang, R. *et al. Cell* **78,** 335–342 (1994).
3. Tavormina, P. L. *et al. Am. J. Hum. Genet.* **64,** 722–731 (1999).
4. Laederich, M. B. & Horton, W. A. *Curr. Opin. Pediatr.* **22,** 516–523 (2010).
5. Okita, K. *et al. Nature Methods* **8,** 409–412 (2011).
6. Koyama, N. *et al. Stem Cells Dev.* **22,** 102–113 (2013).
7. Yasoda, A. *et al. Nature Med.* **10,** 80–86 (2004).
8. Lorget, F. *et al. Am. J. Hum. Genet.* **91,** 1108–1114 (2012).
9. Eiland, L. S. & Luttrell, P. K. *J. Pediatr. Pharmacol. Ther.* **15,** 160–172 (2010).
10. Braamskamp, M. J. *et al. Circulation* **128,** A17837 (2013).
11. Hatano, H., Maruo, A., Bolander, M. E. & Sarkar, G. *J. Orthop. Sci.* **8,** 842–848 (2003).
12. Simopoulou, T., Malizos, K. N., Poultsides, L. & Tsezou, A. *J. Orthop. Res.* **28,** 110–115 (2010).
13. Hunter, A. G., Hecht, J. T. & Scott, C. I. Jr *Am. J. Med. Genet.* **62,** 255–261 (1996).
14. Wynn, J., King, T. M., Gambello, M. J., Waller, D. K. & Hecht, J. T. *Am. J. Med. Genet. A* **143A,** 2502–2511 (2007).
15. Collipp, P. J., Sharma, R. K., Thomas, J., Maddaiah, V. T. & Chen, S. Y. *Am. J. Dis. Child.* **124,** 682–685 (1972).

ARTICLE

doi:10.1038/nature13775

Statin treatment rescues FGFR3 skeletal dysplasia phenotypes

Akihiro Yamashita[1], Miho Morioka[1], Hiromi Kishi[1], Takeshi Kimura[1,2], Yasuhito Yahara[1], Minoru Okada[1], Kaori Fujita[1], Hideaki Sawai[3], Shiro Ikegawa[4] & Noriyuki Tsumaki[1,5]

Gain-of-function mutations in the fibroblast growth factor receptor 3 gene (*FGFR3*) result in skeletal dysplasias, such as thanatophoric dysplasia and achondroplasia (ACH). The lack of disease models using human cells has hampered the identification of a clinically effective treatment for these diseases. Here we show that statin treatment can rescue patient-specific induced pluripotent stem cell (iPSC) models and a mouse model of FGFR3 skeletal dysplasia. We converted fibroblasts from thanatophoric dysplasia type I (TD1) and ACH patients into iPSCs. The chondrogenic differentiation of TD1 iPSCs and ACH iPSCs resulted in the formation of degraded cartilage. We found that statins could correct the degraded cartilage in both chondrogenically differentiated TD1 and ACH iPSCs. Treatment of ACH model mice with statin led to a significant recovery of bone growth. These results suggest that statins could represent a medical treatment for infants and children with TD1 and ACH.

Achondroplasia (ACH) is the most common skeletal dysplasia, and the condition leads to disproportionate short-limb dwarfism. Mutations in the gene encoding fibroblast growth factor receptor 3 (FGFR3) were identified in patients with ACH (refs 1, 2). *FGFR3* mutations were subsequently found in patients with thanatophoric dysplasia, of which there are two types that can be distinguished by the radiographic findings and the results of a molecular analysis: thanatophoric dysplasia type I (TD1) and II (TD2). The phenotype of thanatophoric dysplasia is more severe than that of ACH, and the condition is lethal due to respiratory insufficiency, which is secondary to an abnormal chest wall skeleton. Owing to recent progress in respiratory management, infants with thanatophoric dysplasia can survive for several months to years. *FGFR3* mutations have also been found in some other conditions, which are collectively called FGFR3 chondrodysplasias[3]. Mice that are deficient for FGFR3 show skeletal overgrowth[4]. This mouse phenotype suggests that FGFR3 is a negative regulator of endochondral bone formation, confirming that the mutations causing FGFR3 chondrodysplasias are gain-of-function mutations.

FGFR3 functions as a transmembrane receptor tyrosine kinase. Therapeutic strategies aimed at decreasing excessive FGFR3 signals have been investigated[5]. The application of c-type natriuretic peptide (CNP)[6], a CNP analogue[7], parathyroid hormone[8], a FGFR3-binding peptide[9] and soluble FGFR3 (ref. 10) led to a recovery of bone growth in a genetically manipulated mouse model of FGFR3 chondrodysplasia. CNP attenuates the mitogen-activated protein kinase (MAPK) signals which are activated by FGFR3. The efficacy of all of these treatments remains to be tested in appropriate human cell models, which have not been available for FGFR3 chondrodysplasia. In addition, the safety of these treatments needs to be confirmed through additional pre-clinical and clinical tests before wide clinical use can be advocated. The mechanism(s) by which FGFR3 mutations cause cartilage abnormalities have been investigated by transducing cells with mutant *FGFR3 in vitro*, and generating a genetically engineered mouse model *in vivo*[5]. The former approach provides information on the impact of *FGFR3* mutations on the receptors, such as receptor stabilization and turnover[11]. The latter approach has revealed the impact of *FGFR3* mutations on the growing skeleton and indicated that the endochondral bone formation process is disturbed[12]. In addition to these two approaches, recent progress in cell reprogramming technologies is beginning to offer a new disease model: induced pluripotent stem cells (iPSCs). The iPSCs are generated from dermal fibroblasts or blood cells from patients, followed by differentiation into cell types of interest, such as chondrocytes in the case of FGFR3 chondrodysplasias. This process may provide human cell types and tissues that can allow investigation of the mechanism(s) underlying the onset and progression of disease, and drug screening.

Generation of TD1-specific iPSCs

Human dermal fibroblasts (HDFs) were obtained from three TD1 patients (TD1-714, TD1-10749 and TD1-315H) (Extended Data Fig. 1a). A sequencing analysis of the genomic DNA extracted from the patients' HDFs revealed a heterozygous mutation (R248C) in the *FGFR3* gene in all three TD1 patients (Extended Data Fig. 1a). We established more than three iPSC lines for each TD1 patient and analysed one TD1 iPSC line (TD1-714-3, TD1-10749-1 and TD1-315H-2) derived from the HDFs of each patient. Wild-type iPSC lines (409B2 (ref. 13), KF4009-1 and HDF-11) derived from three control individuals were prepared. We confirmed that all iPSC lines expressed SSEA4 and TRA1-60, and formed teratomas containing all three germ layers (Extended Data Fig. 1a–c).

Abnormal cartilage formation from TD1 iPSCs

We differentiated TD1 and wild-type iPSCs towards chondrocytes. The iPSCs were differentiated into chondrogenic cells in the presence of chondrogenic supplementation on dishes for 14 days, and then were transferred into suspension culture to form cartilaginous particles following the previously described method[14], with modifications. The wild-type iPSCs formed particles composed of cells scattered in a cartilaginous extracellular matrix, as indicated by positive Safranin O staining on day 42. TD1 iPSCs formed particles that did not appear to be stained with Safranin O, indicating that the extracellular matrix contained little glycosaminoglycan (Fig. 1a and Extended Data Fig. 2). The presence of glycosaminoglycan

[1]Cell Induction and Regulation Field, Department of Cell Growth and Differentiation, Center for iPS Cell Research and Application, Kyoto University, Kyoto 606-8507, Japan. [2]Department of Pediatrics, Osaka University Graduate School of Medicine, Osaka 565-0871, Japan. [3]Department of Obstetrics and Gynecology, Hyogo College of Medicine, Hyogo 663-8501, Japan. [4]Laboratory of Bone and Joint Diseases, Center for Integrated Medical Sciences, RIKEN, Tokyo 108-8639, Japan. [5]Japan Science and Technology Agency, CREST, Tokyo 102-0075, Japan.

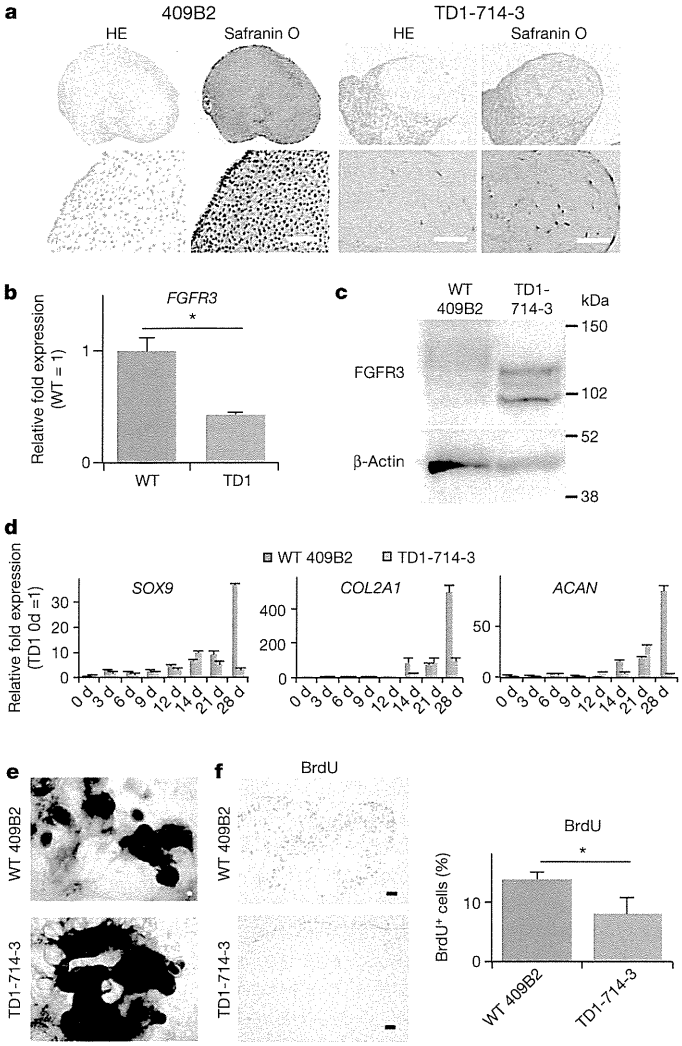

Figure 1 | Chondrogenic differentiation of wild-type iPSCs and TD1 iPSCs. **a**, Histology of iPSC-derived cartilaginous particles on day 42. The images are representative of three independent experiments. HE, haematoxylin and eosin staining. **b**, Results of a real-time RT–PCR expression analysis of *FGFR3* mRNA in chondrogenically differentiated iPSC lines on day 28 ($n = 3$ independent iPSC lines). WT, wild type. **c**, Results of an immunoblot analysis of the FGFR3 protein in chondrogenically differentiated iPSCs on day 28. The images are representative of three independent experiments. **d**, Time course of the changes in the expression of markers in iPSCs subjected to chondrogenic differentiation, as determined by real-time RT–PCR ($n = 3$ technical replicates). **e**, Phase microscopic images of chondrogenically differentiated iPSCs in adhesion culture on day 14. The images are representative of three independent experiments. **f**, iPSC-derived cartilaginous particles on day 28 were treated with BrdU. Left: histological sections were immunostained with anti-BrdU antibodies. Right: the number of BrdU-positive cells were divided by the total number of cells ($n = 3$ particles). The data are representative of two independent experiments. The error bars denote the means ± s.d. $^*P < 0.05$ by the *t*-test. Scale bars, 50 μm.

is important for the mechanical properties of cartilage. Messenger RNA expression analysis showed that there were decreased expression levels of chondrocyte markers and increased expression levels of type I collagen genes in chondrogenically differentiated TD1 iPSCs on day 28 (Extended Data Fig. 3a). Immunohistochemical analysis showed that the TD1-iPSC-derived particles expressed more type I collagen and less type II collagen than the wild-type-iPSC-derived particles on day 42 (Extended Data Fig. 3b, c). Focal deposition of type II collagen in the TD1-iPSC-derived particles (Extended Data Fig. 3c, lower panels) suggests that there was limited cartilage formation or remnant cartilage which was formed in earlier stages that was subsequently degraded. Markers of pluripotency (SSEA4 and TRA1-60) were not detected in either the chondrogenically differentiated wild-type or TD1 iPSCs on day 42 (Extended Data Fig. 3d). The expression level of *FGFR3* mRNA in chondrogenically differentiated TD1 iPSCs was significantly lower than in chondrogenically differentiated wild-type iPSCs (Fig. 1b), probably because of the negative feedback transcriptional regulation due to the gain-of-function mutation of *FGFR3* in the TD1 cells. Immunoblot analysis showed that the amount of FGFR3 protein in the chondrogenically differentiated TD1 iPSCs was higher than in the chondrogenically differentiated wild-type iPSCs (Fig. 1c), supporting the notion that the mutant FGFR3 receptor is resistant to degradation, leading to persistent activation of the receptor's signal transduction[11,15–17].

To examine how the chondrogenic differentiation of TD1 iPSCs resulted in the formation of abnormal particles, we analysed the time course of the changes in expression of markers in wild-type iPSCs and TD1 iPSCs subjected to chondrogenic differentiation (Fig. 1d and Extended Data Fig. 4a). Expression of *OCT4* (also called *POU5F1*), a marker of pluripotency, decreased rapidly on day 3, and expression of mesendodermal/mesodermal markers *T* and *KDR* was transiently increased around days 3–9 in both chondrogenically differentiated wild-type and TD1 iPSCs. Expression of chondrogenic transcription factors *SOX9*, *SOX5* and *SOX6* was activated and increased gradually in both chondrogenically differentiated wild-type and TD1 iPSCs until day 14. Expression levels of *SOX9*, *SOX5* and *SOX6* continued to increase in the chondrogenically differentiated wild-type iPSCs, whereas they decreased gradually after day 14 in the chondrogenically differentiated TD1 iPSCs.

The expression of these chondrogenic transcription factors was followed by expression of their target genes encoding cartilage matrix proteins. Expression of type II collagen gene (*COL2A1*) and aggrecan gene (*ACAN*) was activated on day 14, and increased gradually in both chondrogenically differentiated wild-type and TD1 iPSCs until day 21. The expression levels of *COL2A1* and *ACAN* continued to increase until day 28 in chondrogenically differentiated wild-type iPSCs, whereas they were not changed or were decreased on day 28 in chondrogenically differentiated TD1 iPSCs. These findings suggest that both wild-type iPSCs and TD1 iPSCs were similarly differentiated into chondrocytes until days 14–21. This interpretation was supported by phase microscopic observation, which revealed that the wild-type iPSC and TD1 iPSC cultures similarly produced cell nodules by day 14 (Fig. 1e), because the formation of cell nodules is a typical characteristic of cultured chondrocytes.

Reduced expression of cartilage matrix genes (*COL2A1* and *ACAN*) on day 28, however, indicated that chondrocyte maturation was disturbed in the chondrogenically differentiated TD1 iPSCs after their differentiation into chondrocytes. Previous studies have revealed that chondrocyte proliferation is disturbed in ACH model mice[12] and in chondrocytic cells transduced with *FGFR3* carrying thanatophoric dysplasia and ACH mutations[18], and that chondrocyte apoptosis is increased in thanatophoric dysplasia patients and in chondrogenic cells transduced with *FGFR3* carrying thanatophoric dysplasia and ACH mutations[16,19,20]. Labelling cells with 5-bromodeoxyuridine (BrdU) revealed that the proliferation rate of the chondrogenically differentiated TD1 iPSCs was decreased compared with that of the chondrogenically differentiated wild-type iPSCs on day 28 (Fig. 1f). The chondrogenically differentiated TD1 iPSCs showed increased numbers of TUNEL-positive cells (Extended Data Figs 4 b, c) and increased immunoreactivity for cleaved-caspase 3 (Extended Data Fig. 4d), suggesting that they had increased apoptosis compared with chondrogenically differentiated wild-type iPSCs. Chondrogenically differentiated TD1 iPSCs showed increased expression levels of p21 (Extended Data Fig. 4e). Together these results suggest that the chondrogenically differentiated TD1 iPSC model recapitulates the two primary abnormalities which are found in FGFR3-related disease patients and models: decreased proliferation and increased apoptosis of chondrocytes. These two abnormalities might be responsible for the degraded cartilage tissue found in TD1-iPSC-derived particles on day 42.

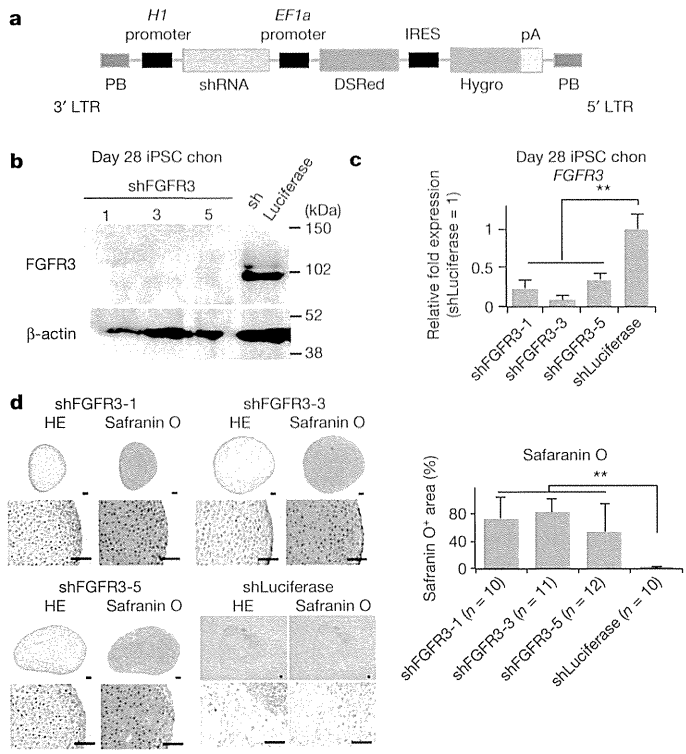

Figure 2 | Results of an analysis of *FGFR3* knockdown in TD1 iPSCs (TD1-714-3) subjected to chondrogenic differentiation. The data were collected from three independent clones respectively bearing three different *FGFR3* shRNAs. **a**, The *FGFR3* shRNA piggyBac (PB) vector. **b**, Results of an immunoblot analysis of FGFR3 on day 28. iPSC chon, chondrogenically differentiated iPSCs. **c**, The results of a real-time RT–PCR expression analysis of *FGFR3* on day 28 ($n = 3$ technical replicates). **d**, Histological analysis on day 42. Scale bars, 50 μm. The right panel shows the area of the Safranin-O-positive region in the particles. The number of particles examined is indicated at the bottom. Error bars denote the means ± s.d. $^{**}P < 0.01$ by the Tukey–Kramer post-hoc test.

FGFR3 inactivation rescues TD1 iPSC cartilage

To confirm that TD1 iPSCs cannot produce cartilaginous particles due to the gain-of-function mutation of *FGFR3*, we knocked down *FGFR3* in TD1 iPSCs (TD1-714-3) using piggyBac short hairpin RNA (shRNA) vectors (Fig. 2a). Expression of *FGFR3* mRNA and protein was effectively knocked down in the chondrogenically differentiated TD1 iPSCs bearing each of three types of *FGFR3* shRNA (Fig. 2b, c). The TD1 iPSCs transfected with *FGFR3* shRNA formed cartilaginous particles that were positively stained by Safranin O (Fig. 2d). Expression analysis showed that chondrogenically differentiated TD1 iPSCs transduced with *FGFR3* shRNA had increased expression of chondrocyte marker genes and decreased expression of fibroblast marker genes compared with chondrogenically differentiated TD1 iPSCs bearing control shRNA targeting the luciferase gene sequence (Extended Data Fig. 5a).

Furthermore, treatment of chondrogenically differentiated TD1 iPSCs with FGFR3 neutralizing antibody resulted in partial recovery of cartilage formation (Extended Data Fig. 5b). Expression analysis showed that addition of the FGFR3 neutralizing antibody increased the expression of chondrocyte marker genes and decreased the expression of fibroblast marker genes in the chondrogenically differentiated TD1 iPSCs (Extended Data Fig. 5c).

These results suggest that the formation of degraded cartilage by TD1 iPSCs is caused by the gain-of-function mutation of *FGFR3*.

Statins rescue TD1-iPSC-derived cartilage

To find effective drugs to treat FGFR3 chondrodysplasias, we screened molecules for their ability to rescue chondrogenically differentiated TD1 iPSCs from the degraded cartilage phenotype. We selected molecules that had previously been reported to affect FGFR3 signalling and/or chondrocyte differentiation. Chondrogenically differentiated TD1 iPSCs were rescued by the addition of CNP but not by the addition of an FGFR inhibitor or the G-protein antagonist NF449 (Extended Data Fig. 6).

We included statins in the candidate molecules because they have been reported to have anabolic effects on chondrocytes[21–23]. The statins compose a drug class broadly characterized as lipid-lowering agents. Statins inhibit mevalonic acid synthesis, and as a consequence lead to a decrease in the amount of total cholesterol and decreased levels of low-density lipoproteins. Statins have favourable effects on cardiovascular disease, the nervous system, the immune system, the skeletal system and tumour growth[24–27], and there is emerging interest in the pleiotropic

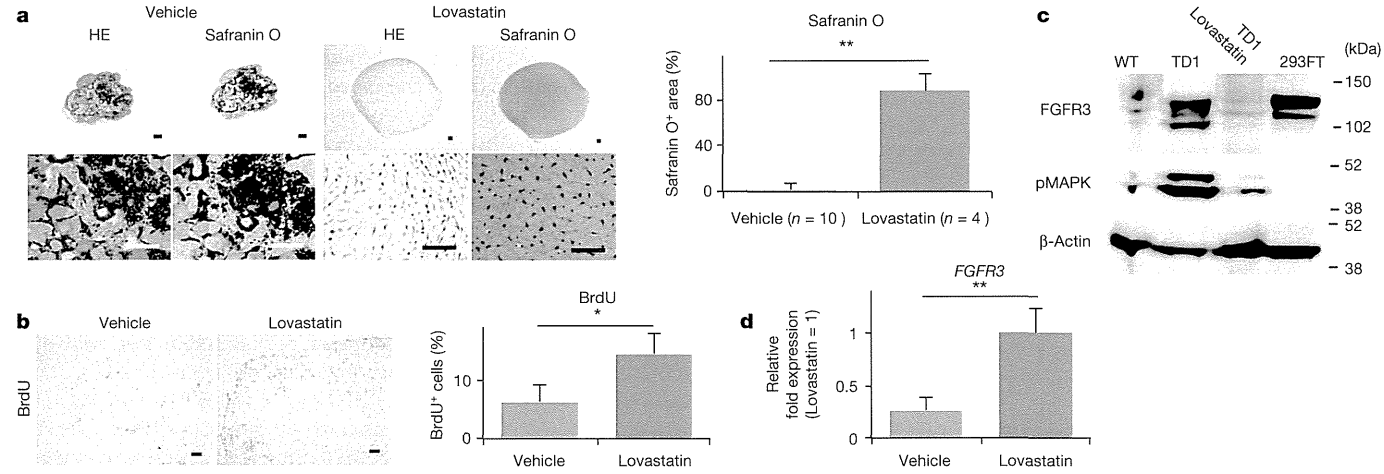

Figure 3 | TD1 (TD1-714-3) iPSCs were chondrogenically differentiated to produce particles in the presence or absence of lovastatin (1 μM). **a**, Left: histology of the particles on day 42. Right: area of the Safranin-O-positive region in the particles. The number of particles examined is indicated at the bottom. The data are representative of three independent experiments. **b**, Particles on day 28 were treated with BrdU. Left: histological sections were immunostained with anti-BrdU antibodies. Right: number of BrdU-positive cells were divided by the total number of cells ($n = 3$ particles). The data are representative of two independent experiments. **c**, Results of an immunoblot analysis of FGFR3 and phosphorylated MAPK on day 28. WT, wild-type (409B2)-iPSC-derived particles. 293FT, 293FT cells. The images are representative of three independent experiments. **d**, Results of a real-time RT–PCR expression analysis of *FGFR3* on day 28 ($n = 3$ technical replicates). The data are representative of two independent experiments. Error bars denote the means ± s.d. $^{*}P < 0.5$; $^{**}P < 0.01$ by the *t*-test. Scale bars, 50 μm.

effects of statins. We found that the addition of lovastatin recovered the cartilage formation of chondrogenically differentiated TD1 iPSCs (Fig. 3a). An expression analysis showed that the addition of lovastatin increased the expression of a chondrogenic transcription factor (*SOX9*) and cartilage extracellular components (*COL2A1* and *ACAN*) in chondrogenically differentiated TD1 iPSCs (Extended Data Fig. 7a). Labelling TD1-iPSC-derived particles cultured in the presence or absence of lovastatin with BrdU revealed that the addition of lovastatin increased the proliferation rates of chondrogenically differentiated TD1 iPSCs in the particles (Fig. 3b). Furthermore, we confirmed that addition of mevastatin, atorvastatin, pravastatin, rosuvastatin and fluvastatin also recovered the cartilage formation of chondrogenically differentiated TD1 iPSCs (Extended Data Fig. 7b). These results suggest that various statins can rescue chondrogenically differentiated TD1 iPSCs.

To gain insight into the mechanism(s) by which statins rescue the FGFR3 chondrodysplasia models, we examined the expression levels of FGFR3 protein and mRNA. Immunoblot analysis revealed that application of lovastatin rescued chondrogenically differentiated TD1 iPSCs from the increased amount of FGFR3 protein (Fig. 3c). Accordingly, application of lovastatin rescued chondrogenically differentiated TD1 iPSCs from an increased amount of phosphorylated MAPK, a downstream target of FGFR3 signalling. The changes in the amount of FGFR3 protein were not regulated at the mRNA expression level, because the *FGFR3* mRNA expression levels were increased by lovastatin application in chondrogenically differentiated TD1 iPSCs (Fig. 3d), suggesting that statin treatment may accelerate the degradation of FGFR3 protein in chondrogenically differentiated TD1 iPSCs.

Statin exposure rescues ACH iPSC cartilage

We next investigated whether lovastatin could rescue another FGFR3 chondrodysplasia: ACH. We generated iPSCs from HDFs obtained from two individuals with ACH and one individual who was homozygous for an ACH mutation (ACHhomo). The chondrogenic differentiation of ACH iPSCs and ACHhomo iPSCs resulted in the formation of particles that lacked the cartilaginous element, as indicated by negative Safranin O staining. Addition of lovastatin to the culture media recovered the cartilage formation of chondrogenically differentiated ACH iPSCs and ACHhomo iPSCs (Extended Data Fig. 8).

Statins cause bone elongation in ACH mice

We examined whether statin treatment could rescue *Fgfr3*^{Ach} transgenic mice from the FGFR3 chondrodysplasia phenotype *in vivo*. The *Fgfr3*^{Ach} transgenic mice[12] express *Fgfr3* with an ACH mutation in chondrocytes under the control of the *Col2a1* promoter/enhancer sequences. *Fgfr3*^{Ach} transgenic mice show dwarfism, short limb bones and a short snout. Daily intraperitoneal injections of rosuvastatin significantly increased the anteroposterior lengths of the skulls and the lengths of the ulnas, femurs and tibiae in the *Fgfr3*^{Ach} mice when they were 15 days old (Fig. 4 and Extended Data Fig. 9). There were no significant differences in the lengths of the ulnas and tibiae between *Fgfr3*^{Ach} mice receiving rosuvastatin and wild-type mice receiving vehicle.

The lengths of primordial cartilage in *Fgfr3*^{Ach} mice increased more in organ culture in the presence of lovastatin than in the absence of lovastatin (Extended Data Fig. 10a), indicating that lovastatin acts on the cartilage directly to induce its elongation. Labelling the primordial cartilage with BrdU revealed that lovastatin increased the proliferation rate of chondrocytes in the *Fgfr3*^{Ach} primordial cartilage (Extended Data Fig. 10b).

The pellets of *Fgfr3*^{Ach} primary chondrocytes cultured in the presence of lovastatin showed more intense Safranin O staining than did the pellets of *Fgfr3*^{Ach} primary chondrocytes in the absence of lovastatin (Extended Data Fig. 10c). *Fgfr3*^{Ach} pellets cultured in the presence of lovastatin showed increased expression levels of *Sox9*, *Col2a1* and *Acan* at 2 weeks after the start of pellet culture, as well as increased expression levels of *Runx2* and *Col10a1* at 4 weeks after the start of pellet culture, compared with those cultured in the absence of lovastatin (Extended Data Fig. 10d). These results suggest that statin treatment stimulated both chondrocytic differentiation and maturation towards hypertrophy by increasing the expression of *Sox9* and *Runx2*, respectively.

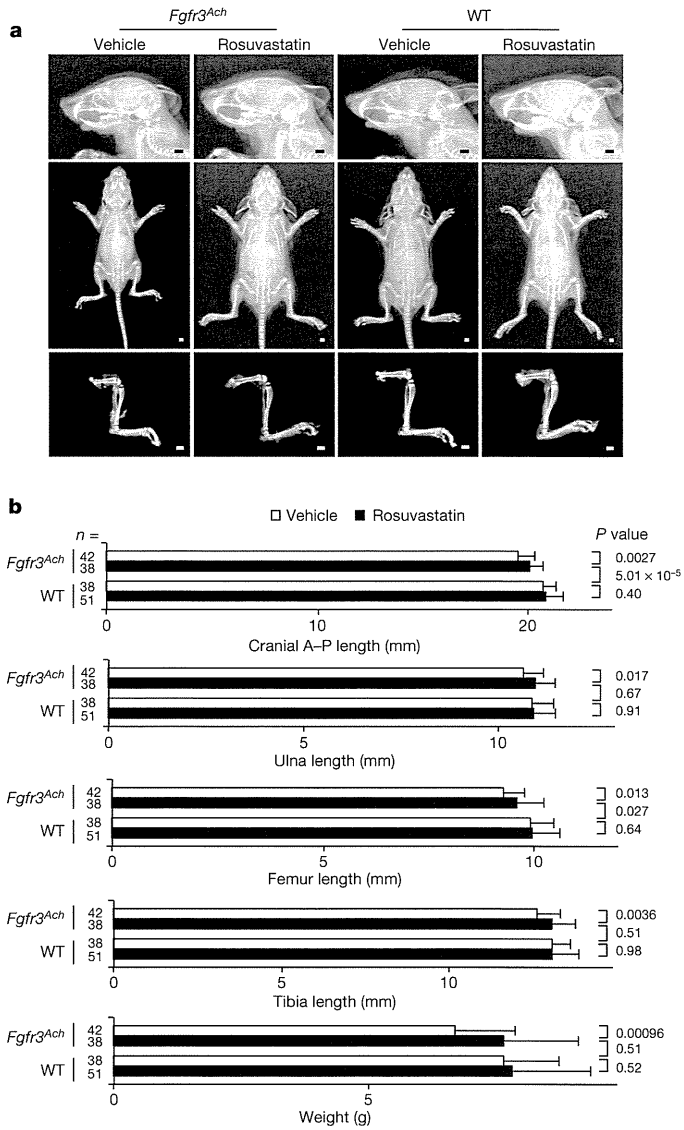

Figure 4 | Rescuing ACH model (*Fgfr3*^{Ach}) mice from reduced bone growth by intraperitoneal injection of rosuvastatin. **a**, Top: X-ray images of heads. Lateral views. Middle: X-ray images of bodies. Anterior–posterior view. Bottom: X-ray images of the hindlimb skeletons. Scale bars, 2 mm. **b**, Measurements of the anteroposterior (A–P) length of the heads and the length of the ulnas, femurs and tibiae in X-ray images and weights. The numbers of mice for each group were: *Fgfr3*^{Ach} mice treated with vehicle, $n = 42$; *Fgfr3*^{Ach} mice treated with statin, $n = 38$; wild-type mice treated with vehicle, $n = 38$; wild-type mice treated with statin, $n = 51$. The error bars denote the means ± s.d. *t*-test *P* values are indicated.

Immunoblot analysis of primary chondrocytes showed that a larger amount of FGFR3 was detected in the *Fgfr3*^{Ach} chondrocytes than in the wild-type chondrocytes (Extended Data Fig. 10e), probably due to overexpression of the *Fgfr3*^{Ach} transgene and inhibited degradation of the mutant FGFR3. Addition of lovastatin to the culture decreased the amount of FGFR3 in the *Fgfr3*^{Ach} chondrocytes, and addition of MG132 increased the amount of FGFR3 in *Fgfr3*^{Ach} chondrocytes which were cultured in the presence of lovastatin. The expression of FGFR3 was slightly increased in *Fgfr3*^{Ach} chondrocytes by the addition of bafilomycin A1 in the presence of lovastatin in the cultures. These results suggest that statin treatment induced the degradation of mutant FGFR3, mainly through a proteasomal pathway.

Discussion

The degree of abnormality in the histology of the resultant TD1-iPSC- and ACH-iPSC-derived cartilaginous particles on day 42 appeared to be more severe than that observed in the cartilage of patients with TD1 and ACH, respectively. One of the reasons for this discrepancy may be that the *in vitro* culture environment lacks any compensatory machinery to adapt skeletal tissues to the malfunction of chondrocytes caused by FGFR3 mutations. The exaggeration of phenotypes has been recognized in iPSC models of other diseases, including Alzheimer's disease[28]. This exaggeration of the phenotype exhibited by TD1-iPSC-derived chondrocytes may be advantageous for screening drugs, because it may decrease the occurrence of false-negative events.

We injected ACH model mice with 1.0 mg kg^{-1} rosuvastatin, which is equivalent to 70 mg per day in a 70 kg human. A dose of 80 mg per day of rosuvastatin was studied in a clinical trial and found to be associated with an increased risk of muscle toxicity and renal toxicity compared with a dose of 40 mg per day[29]. However, a dose of 1.0 mg per kg rosuvastatin is not always intolerable. It is important to note that when rosuvastatin was administered at this dose it was able to elongate the skeletal elements of the ACH model mice, because a considerable proportion of the statin administered was removed by the liver. It remains to be determined which statin is the most effective and what dose is needed. The precise mechanism(s) by which statin treatment can rescue the chondrocyte abnormalities associated with FGFR3 diseases remain to be elucidated, although we have obtained some insights into the statin-induced promotion of FGFR3 degradation, which is inhibited in cases with mutant FGFR3 (see Supplementary Discussion for further information).

Because statins have been administered to large numbers of human patients for many years, there is abundant information available on their safety, although their effects on infants and juvenile patients are still largely unknown. The fact that the treatment rescued both human iPSC disease models and mouse disease models suggests that statins might be effective and applicable for patients with TD1 and ACH.

Online Content Methods, along with any additional Extended Data display items and Source Data, are available in the online version of the paper; references unique to these sections appear only in the online paper.

Received 1 February; accepted 19 August 2014.
Published online 17 September 2014.

1. Rousseau, F. *et al.* Mutations in the gene encoding fibroblast growth factor receptor-3 in achondroplasia. *Nature* **371,** 252–254 (1994).
2. Shiang, R. *et al.* Mutations in the transmembrane domain of FGFR3 cause the most common genetic form of dwarfism, achondroplasia. *Cell* **78,** 335–342 (1994).
3. Warman, M. L. *et al.* Nosology and classification of genetic skeletal disorders: 2010 revision. *Am. J. Med. Genet. A.* **155,** 943–968 (2011).
4. Deng, C., Wynshaw-Boris, A., Zhou, F., Kuo, A. & Leder, P. Fibroblast growth factor receptor 3 is a negative regulator of bone growth. *Cell* **84,** 911–921 (1996).
5. Laederich, M. B. & Horton, W. A. Achondroplasia: pathogenesis and implications for future treatment. *Curr. Opin. Pediatr.* **22,** 516–523 (2010).
6. Yasoda, A. *et al.* Systemic administration of C-type natriuretic peptide as a novel therapeutic strategy for skeletal dysplasias. *Endocrinology* **150,** 3138–3144 (2009).
7. Lorget, F. *et al.* Evaluation of the therapeutic potential of a CNP analog in a Fgfr3 mouse model recapitulating achondroplasia. *Am. J. Hum. Genet.* **91,** 1108–1114 (2012).
8. Xie, Y. *et al.* Intermittent PTH (1–34) injection rescues the retarded skeletal development and postnatal lethality of mice mimicking human achondroplasia and thanatophoric dysplasia. *Hum. Mol. Genet.* **21,** 3941–3955 (2012).
9. Jin, M. *et al.* A novel FGFR3-binding peptide inhibits FGFR3 signaling and reverses the lethal phenotype of mice mimicking human thanatophoric dysplasia. *Hum. Mol. Genet.* **21,** 5443–5455 (2012).
10. Garcia, S. *et al.* Postnatal soluble FGFR3 therapy rescues achondroplasia symptoms and restores bone growth in mice. *Sci. Transl Med.* **5,** 203ra124 (2013).
11. Monsonego-Ornan, E., Adar, R., Feferman, T., Segev, O. & Yayon, A. The transmembrane mutation G380R in fibroblast growth factor receptor 3 uncouples ligand-mediated receptor activation from down-regulation. *Mol. Cell. Biol.* **20,** 516–522 (2000).
12. Naski, M. C., Colvin, J. S., Coffin, J. D. & Ornitz, D. M. Repression of hedgehog signaling and BMP4 expression in growth plate cartilage by fibroblast growth factor receptor 3. *Development* **125,** 4977–4988 (1998).
13. Okita, K. *et al.* A more efficient method to generate integration-free human iPS cells. *Nature Methods* **8,** 409–412 (2011).
14. Oldershaw, R. A. *et al.* Directed differentiation of human embryonic stem cells toward chondrocytes. *Nature Biotechnol.* **28,** 1187–1194 (2010).
15. Cho, J. Y. *et al.* Defective lysosomal targeting of activated fibroblast growth factor receptor 3 in achondroplasia. *Proc. Natl Acad. Sci. USA* **101,** 609–614 (2004).
16. Harada, D. *et al.* Sustained phosphorylation of mutated FGFR3 is a crucial feature of genetic dwarfism and induces apoptosis in the ATDC5 chondrogenic cell line via PLCγ-activated STAT1. *Bone* **41,** 273–281 (2007).
17. Guo, C. *et al.* Sprouty 2 disturbs FGFR3 degradation in thanatophoric dysplasia type II: a severe form of human achondroplasia. *Cell. Signal.* **20,** 1471–1477 (2008).
18. Krejci, P. *et al.* Analysis of STAT1 activation by six FGFR3 mutants associated with skeletal dysplasia undermines dominant role of STAT1 in FGFR3 signaling in cartilage. *PLoS ONE* **3,** e3961 (2008).
19. Legeai-Mallet, L., Benoist-Lasselin, C., Delezoide, A. L., Munnich, A. & Bonaventure, J. Fibroblast growth factor receptor 3 mutations promote apoptosis but do not alter chondrocyte proliferation in thanatophoric dysplasia. *J. Biol. Chem.* **273,** 13007–13014 (1998).
20. Yamanaka, Y., Tanaka, H., Koike, M., Nishimura, R. & Seino, Y. PTHrP rescues ATDC5 cells from apoptosis induced by FGF receptor 3 mutation. *J. Bone Miner. Res.* **18,** 1395–1403 (2003).
21. Yudoh, K. & Karasawa, R. Statin prevents chondrocyte aging and degeneration of articular cartilage in osteoarthritis (OA). *Aging* **2,** 990–998 (2010).
22. Simopoulou, T., Malizos, K. N., Poultsides, L. & Tsezou, A. Protective effect of atorvastatin in cultured osteoarthritic chondrocytes. *J. Orthop. Res.* **28,** 110–115 (2010).
23. Baker, J. F., Walsh, P. M., Byrne, D. P. & Mulhall, K. J. Pravastatin suppresses matrix metalloproteinase expression and activity in human articular chondrocytes stimulated by interleukin-1β. *J. Orthopaed. Traumatol.* **13,** 119–123 (2012).
24. Mundy, G. *et al.* Stimulation of bone formation *in vitro* and in rodents by statins. *Science* **286,** 1946–1949 (1999).
25. Millar, P. J. & Floras, J. S. Statins and the autonomic nervous system. *Clinical Sci.* **126,** 401–415 (2014).
26. Olivieri, F. *et al.* Telomere/telomerase system: a new target of statins pleiotropic effect? *Curr. Vasc. Pharmacol.* **10,** 216–224 (2012).
27. Zhang, J. *et al.* Statins, autophagy and cancer metastasis. *Int. J. Biochem. Cell Biol.* **45,** 745–752 (2013).
28. Israel, M. A. *et al.* Probing sporadic and familial Alzheimer's disease using induced pluripotent stem cells. *Nature* **482,** 216–220 (2012).
29. Wolfe, S. M. Dangers of rosuvastatin identified before and after FDA approval. *Lancet* **363,** 2189–2190 (2004).

Supplementary Information is available in the online version of the paper.

Acknowledgements We thank H. Ohashi, J. Murotsuki, T. Yamada and K. Ozono for preparation of the dermal fibroblasts from a patient and discussion. We thank D. Ornitz and A. Yasoda for the *Fgfr3*^{Ach} mice. We thank K. Okita and S. Yamanaka for providing the hiPSC line 409B2, and A. Hotta for transducing the piggyBac vectors. We thank A. Motomura, X. Chen, Y. Minegishi, M. Nishino, T. Kobayashi, N. Oda, E. Ikeda and Y. Makita for their assistance. This study was supported in part by the Japan Science Technology Agency (JST), CREST (to N.T.) and Research Center Network for Realization of Regenerative Medicine (to N.T.), and Scientific Research Grant No. 24890101 (to A.Y.) and 26861716 (to A.Y.) and No. 24390354 (to N.T.) from MEXT.

Author Contributions A.Y. was involved in most of the experiments. M.M. performed the immunohistological and immunoblot analyses, as well as the DNA construction. H.K., T.K. and Y.Y. performed the mouse experiments. M.O. contributed to the generation of iPSCs. H.S. and S.I. were involved in the study design. K.F. performed the immunoblot analyses. N.T. designed the study. A.Y. and N.T. wrote the paper.

Author Information Reprints and permissions information is available at www.nature.com/reprints. The authors declare no competing financial interests. Readers are welcome to comment on the online version of the paper. Correspondence and requests for materials should be addressed to N.T. (ntsumaki@cira.kyoto-u.ac.jp).

METHODS

Ethics statement. All experiments were approved by the institutional review board, institutional animal committee (as appropriate) and the institutional biosafety committee of Kyoto University.

Generation of patient-specific iPSCs. HDFs derived from six patients (Extended Data Fig. 1a) were obtained from the cell banks of the Coriell Institute and Saitama Children's Medical Center. Control HDFs from two different neonates were purchased from KURABO (strain 01491 and 01439). HDFs were cultured in DMEM (Sigma) with 10% FBS (Invitrogen), 50 U ml^{-1} penicillin and 50 μg ml^{-1} streptomycin. To generate iPSCs, episomal plasmid vectors (Mixture Y4: *OCT4*, *SOX2*, *KLF4*, *L-MYC*, *LIN28* and *p53* shRNA) were electroporated into HDFs with the Neon transfection system (Invitrogen)[13]. One week after transduction, 1×10^5 cells were re-seeded into 100 mm dishes with feeder cells. The cells were subsequently cultured in hiPSC medium. The 409B2 cells used as the control iPSCs were a gift from K. Okita and S. Yamanaka (Center for iPS Cell Research and Application (CiRA), Kyoto University, Kyoto, Japan)[13]. All cells were negative for mycoplasma contamination.

Chondrogenic differentiation of hiPSCs. The hiPSCs were transferred and then maintained in a feeder-free medium, Essential 8 (Invitrogen) with 50 units ml^{-1} penicillin and 50 mg ml^{-1} streptomycin, in 3.5-cm Matrigel-coated dishes. The hiPSCs formed high-density cell colonies which consisted of $1–2 \times 10^5$ cells 10–15 days after the start of maintenance under the feeder-free culture conditions. Subsequently, the chondrogenic differentiation of iPSCs was performed following the previously described method[14], with modifications. The hiPSCs were initially differentiated into mesendodermal cells in DMEM/F12 (Sigma) with 10 ng ml^{-1} of Wnt3A (R&D), 10 ng ml^{-1} of Activin A (R&D), 1% ITS (Invitrogen), 1% FBS and 50 units and 50 mg ml^{-1} of penicillin and streptomycin, respectively (Invitrogen) for 3 days. On day 3, the medium was changed to the basal medium (DMEM (Sigma) with 1% ITS, 1% FBS, 2 mM L-glutamine (Invitrogen), 1×10^{-4} M non-essential amino acids (Invitrogen), 1 mM Na pyruvate (Invitrogen), 50 units of penicillin and 50 mg ml^{-1} of streptomycin) supplemented with 50 μg ml^{-1} of ascorbic acid (Nacalai), 10 ng ml^{-1} of BMP2 (Peprotech), 10 ng ml^{-1} of TGFβ1 (Peprotech) and 10 ng ml^{-1} of GDF5 (PTT), which was intended to commit the cells to the chondrocytic lineage. A total of 10 ng ml^{-1} of bFGF (WAKO) was added to the chondrogenic medium from day 3 to day 14 to increase the cell proliferation. Chondrogenic cells form multilayered nodules by day 14. The nodules were physically separated from the bottom of the dishes to form particles, which were then transferred to a suspension culture in 3.5-cm Petri dishes on day 14. The cells in the particles produce cartilaginous extracellular matrix, resulting in the particles becoming cartilaginous tissue in suspension culture. Particles were harvested on days 28 and 42 for the analyses. The culture medium was changed every 2–7 days.

Histological analysis. The particles in the suspension culture, metatarsals in the organ culture and pellets in the pellet culture were collected, fixed with 4% paraformaldehyde, processed and embedded in paraffin. For some experiments (the results of which are shown in Figs 1f and 3b), the particles were immediately embedded in SCEM compound (SECTION-LAB) and subjected to frozen sectioning according to the method described by Kawamoto[30]. Semi-serial sections were prepared and stained with haematoxylin and eosin (HE) or Safranin-O-fast green-iron haematoxylin (Safranin O) or were immunostained with specific antibodies.

The area of the Safranin-O-positive region and the total area of the particle were measured. The measurements of these areas were performed in a blinded manner. The area of the Safranin-O-positive region was divided by the total area of the particle.

For the anti-type I collagen antibody (Southern Biotech, 1320-01), immune complexes were detected by using N-Histofine Simple Stain MAX PO (GO) (Nichirei Biosciences, 414351) and DAB (DAKO, K3468) as a chromogen. For the anti-SSEA4 antibodies (Santa Cruz, sc-5279), anti-TRA1-60 antibodies (Abcam, ab16287), anti-type II collagen (Thermo MS-235) and cleaved caspase 3 (Cell signalling, Asp175), immune complexes were detected using secondary antibodies conjugated to Alexa Fluor 488 or 546.

For the TUNEL assay, an *in situ* cell death detection kit (TMR red; Roche) was used according to the manufacturer's instructions.

For BrdU labelling, samples were treated with BrdU overnight before collection. The incorporated BrdU was detected using a BrdU staining kit (Invitrogen). The numbers of BrdU-positive cells and total cells were counted in a blinded manner. The number of BrdU-positive cells was divided by the total number of cells.

RNA isolation and quantitative real-time RT–PCR. Total RNA was isolated from whole-cell lysates using the RNeasy Mini kit (Qiagen) according to the manufacturer's instructions with on-column DNase I digestion. The total RNAs prepared from the re-differentiated human fetal chondrocytes were purchased from Cell Applications, Inc. (402RD-R10f). A total of 500 ng of total RNA was used as a template for cDNA synthesis using the ReverTra Ace system (TOYOBO). The amplified products were used to derive standard curves for quantitative real-time PCR. Real-time PCR was performed in a Step One system (ABI) using a KAPA SYBR FAST qPCR kit Master Mix and the ABI prism (KAPA BIOSYSTEMS). The expression levels were normalized to the level of β-actin for human expression studies and *Gapdh* for the mouse mRNA expression levels. The primer sequences are shown in Supplementary Tables 1 and 2.

Immunoblot analysis. Cell lysates were subjected to SDS–PAGE. The separated proteins were then electroblotted and immunostained with the anti-FGFR3 antibody (Cell Signaling, 4574), anti-phosphorylated MAPK antibody (Cell Signaling, 9109) and anti β-actin antibody (Cell Signaling, 49776). FGFR3 migrates on SDS–PAGE as several bands due to the different levels of post-translational modification[11].

***FGFR3* shRNA.** Three short hairpin RNAs (shRNA) targeting different sites of *FGFR3* (shFGFR3-1, -3 and -5) were cloned into piggyBac vectors (Fig. 2a). A shRNA targeting the luciferase sequence was used as a control. The target sequences are shown in Supplementary Table 3. The *FGFR3* shRNA piggyBac vector and transposase expression vector (PBaseII, P16-25)—a gift from A. Hotta (Center for iPS Cell Research and Application (CiRA), Kyoto University, Kyoto, Japan)—were introduced into the TD1-iPSCs (TD1-714-3) using nucleofection technology according to the manufacturer's instructions (Amaxa). TD1 iPSC lines bearing the *FGFR3* shRNA sequence were established.

FGFR3 neutralizing antibody. The FGFR3 neutralizing antibody was purchased from Santa Cruz (sc-13121). A total of 1 μl of the antibody solution was added to 1 ml of cell culture medium (200 ng ml^{-1}) during the chondrogenic differentiation of TD1 iPSCs. As a control, we used IgG (Cell Signaling, #27295), and 1 μl of the IgG solution was added to 1 ml of medium.

Preparation of test molecules. The stock CNP (Sigma, N8768), NF449 (Abcam, ab120415) and FGFR inhibitor (PD 173047, Cayman) solutions were prepared at a concentration of 100 μM, 50 mM and 1 mM, respectively. The final concentrations of CNP, NF449 and the FGFR inhibitor were 100 nM, 25 μM and 1 μM, respectively. The stock lovastatin (TCI, L0214), mevastatin (Cayman, 10010340), atorvastatin (LKT A7658), pravastatin (Cayman, 10010343), rosuvastatin (BioVision, 1995-5) and fluvastatin (Cayman, 10010337) solutions were prepared by dissolving them in DMSO at a concentration of 10 mM. The final concentrations of all statin solutions were 1 μM. Aliquots of stock solutions were added to the culture medium. As a control, an equal amount of water or DMSO was added to the medium (vehicle).

***Fgfr3*^{Ach} mice.** The *Fgfr3*^{Ach} transgenic mice[12] were a gift from D. Ornitz (Washington University School of Medicine). We produced a large number of mice by *in vitro* fertilization[31]. Spermatozoa were collected from male heterozygous *Fgfr3*^{Ach} mice (FVB strain). Oocytes were collected from superovulated wild-type female mice (C57BL/6 mice). The spermatozoa were added to the oocytes. Fertilized oocytes were transferred into pseudopregnant mice (ICR). A total of 172 pups from a total of 13 litters were obtained on the same day. The pups were F_1 hybrid mice, and were genetically uniform. All 172 pups were included in the study. Rosuvastatin was dissolved in phosphate-buffered saline (PBS). A total of seven and six litters, with a total of 90 and 82 pups, were treated with rosuvastatin (1.0 mg kg^{-1}) or vehicle (PBS), respectively. We injected the solution (statin or PBS) into the peritoneal space of pups six times per week from 3 days after birth (day 3) until day 14. One mouse receiving rosuvastatin was found dead on day 14. Mice receiving PBS were found dead on days 3 and day 4 (one mouse each day). The dead mice were thought to have been lost due to having been eaten, and were not able to be subjected to any of the analyses, including genotyping. The remaining 169 mice were killed on day 15, and then were subjected to X-ray imaging (Faxitron DX-50). Measurements of the lengths of skeletal components on X-ray images were performed in a blinded manner. Genomic DNA was extracted from the toes of each mouse and subjected to a genotype analysis, as reported previously[12]. The post-hoc power analysis comparing the *Fgfr3*^{Ach} mice treated with vehicle and the *Fgfr3*^{Ach} mice treated with statin was performed using the G*Power 3.1 software program[32]. The effect size, d, was 0.64, as a function of the two-tailed t-test, with power $(1 - \beta) = 0.8$, $\alpha = 0.05$, $n_1 = 38$ and $n_2 = 42$.

Organ culture of the metatarsal primordial cartilage from *Fgfr3*^{Ach} mice. To examine whether the statin affected the cartilage directly or indirectly, we performed organ culture of metatarsal primordial cartilage prepared from *Fgfr3*^{Ach} transgenic mice in the presence or absence of lovastatin for 7 days. Metatarsals were collected from 15.5 d.p.c. mouse embryos with a mixed FVB × C57BL/6 genetic background, and were subjected to organ culture as described previously[33]. After the genotypes of the pups were determined, the metatarsals from *Fgfr3*^{Ach} embryos were treated with 1 μM lovastatin or vehicle. The measurements of the lengths of the metatarsals were performed in a blinded manner.

Preparation of primary chondrocytes from *Fgfr3*^{Ach} mice. The primary chondrocytes were prepared from newborn mice with a mixed FVB × C57BL/6 genetic background as described previously[34]. After the genotypes of pups were determined, the primary chondrocytes from *Fgfr3*^{Ach} animals or those from wild-type animals were trypsinized and mixed, respectively. The cells were subsequently used for pellet culture to analyse the effects of statin treatment on the differentiation and maturation of *Fgfr3*^{Ach} chondrocytes or were subjected to monolayer culture to analyse the degradation of FGFR3 in *Fgfr3*^{Ach} chondrocytes.

Pellet culture of primary chondrocytes from *Fgfr3^{Ach}* mice. To analyse how the statin affected the differentiation of chondrocytes, we performed pellet culture of the chondrocytes prepared from *Fgfr3^{Ach}* transgenic mice. Chondrocytes normally undergo differentiation and maturation towards hypertrophy in pellet culture. A total of 5×10^5 primary chondrocytes prepared from *Fgfr3^{Ach}* mice were transferred into a 15-ml tube (Falcon) and centrifuged at 200*g* for 10 min[35]. The resulting cell pellet was incubated for 2 or 4 weeks in the presence or absence of 1 μM lovastatin.

Monolayer culture of primary chondrocytes from *Fgfr3^{Ach}* mice in the presence of MG132 or bafilomycin A1. To examine how the statin treatment affected the degradation of the FGFR3 protein, we analysed the effects of a proteasome inhibitor, MG132, and a lysosome inhibitor, bafilomycin A1, on the amounts of FGFR3 protein. We prepared primary chondrocyte cultures from wild-type and *Fgfr3^{Ach}* mice. A total of 2.5×10^5 primary chondrocytes were plated in each well of a six-well plate, and were cultured in the presence or absence of 1 μM lovastatin for 2 days. Next, the culture was supplemented with 10 mM MG132 (Sigma, M7449), 100 nM bafilomycin A1 (Sigma, B1793) or vehicle. Two hours later, the culture was further supplemented with 50 ng ml^{-1} FGF9 (Peprotech) and incubated at 4 °C for 2 h. Then cells were collected and subjected to an immunoblot analysis using an anti-FGFR3 antibody.

Statistical analysis. The data are shown as averages and standard deviations. We used ANOVA followed by the Tukey–Kramer post-hoc test. In Figs 1b, f, 3a, b, d and 4b and in Extended Data Figs 4c, 5c, 10a, b, d, homogenous variances were assumed by the *F* test and the Student's *t*-test (two-sided) was used. *P* values <0.05 were considered to be statistically significant.

30. Kawamoto, T. Use of a new adhesive film for the preparation of multi-purpose fresh-frozen sections from hard tissues, whole-animals, insects and plants. *Arch. Histol. Cytol.* **66,** 123–143 (2003).
31. Takeo, T. *et al.* Birth of mice from vitrified/warmed 2-cell embryos transported at a cold temperature. *Cryobiology* **58,** 196–202 (2009).
32. Faul, F., Erdfelder, E., Lang, A. G. & Buchner, A. G*Power 3: a flexible statistical power analysis program for the social, behavioral, and biomedical sciences. *Behav. Res. Methods* **39,** 175–191 (2007).
33. Ikegami, D. *et al.* Identification of small molecular compounds and fabrication of its aqueous solution by laser-ablation, expanding primordial cartilage. *Osteoarth. Cartil.* **19,** 233–241 (2011).
34. Gosset, M., Berenbaum, F., Thirion, S. & Jacques, C. Primary culture and phenotyping of murine chondrocytes. *Nature Protocols* **3,** 1253–1260 (2008).
35. Hiramatsu, K. *et al.* Generation of hyaline cartilaginous tissue from mouse adult dermal fibroblast culture by defined factors. *J. Clin. Invest.* **121,** 640–657 (2011).

a

iPSC line	Sex	Age at sampling	Race	ID (cell bank) / lot (company)	origin	FGFR3 mutations	iPSCs	
							hESC markers	Teratomas
TD1-714-3	M	1d	Caucasian	GM00714 (Coriell)	Fibroblast	742C>T [Arg248Cys]	Yes	Yes
TD1-10749-2	M	1d	Caucasian	GM10749 (Coriell)	Fibroblast	742C>T [Arg248Cys]	Yes	Yes
TD1-315H-2	F	21 weeks and 4 days gestation	Japanese	S2012 (Saitama[1])	Fibroblast	742C>T [Arg248Cys]	Yes	Yes
ACH-8857-1	M	34y	Caucasian	GM08857 (Coriell)	Fibroblast	1138G>A [Gly380Arg]	Yes	Yes
ACH-8858-6	F	30y	Caucasian	GM08858 (Coriell)	Fibroblast	1138G>A [Gly380Arg]	Yes	Yes
ACHhomo -8859-3	F	1m	Caucasian	GM08859 (Coriell)	Fibroblast	1138G>A [Gly380Arg] homozygous	Yes	Yes
409B2	F	36y	Caucasian	HDF1388	Fibroblast	No	Yes	Yes
KF4009-1	M	Newborn	Asian/ Caucasian	01491 (Kurabo)	Fibroblast	No	Yes	Yes
HDF-11	M	Newborn	Asian	01439 (Kurabo)	Fibroblast	No	Yes	Yes

[1]Saitama, Saitama Children's Medical Center, Japan. [2]CiRA, Center for iPS Cell Research and Application.

b

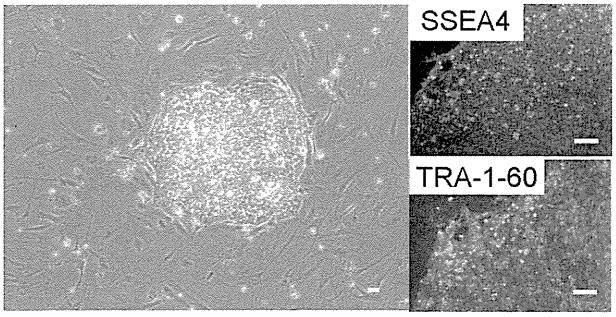

c

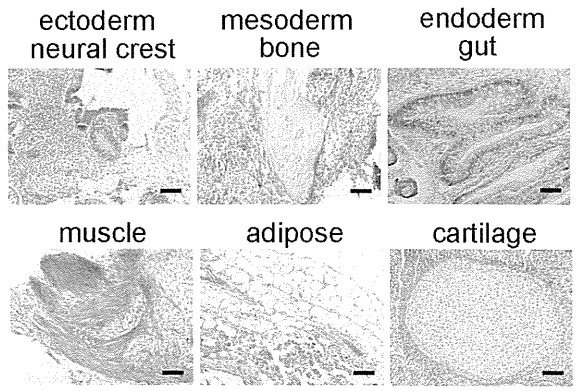

Extended Data Figure 1 | Characterization of the TD1 and ACH iPSCs. **a**, Donor information and characterization of iPSCs. **b**, Left: a phase contrast image of TD1 iPSCs (TD1-714-3). Right: immunocytochemical staining of TD1 iPSCs (TD1-714-3) for SSEA4 and TRA1-60. The images are representative of two independent experiments. **c**, The histology of teratomas formed after implantation of TD1 iPSCs (TD1-10749-2) into SCID mice. The images are representative of experiments using three TD1 iPS clones established from three different patients. Scale bars, 50 μm.

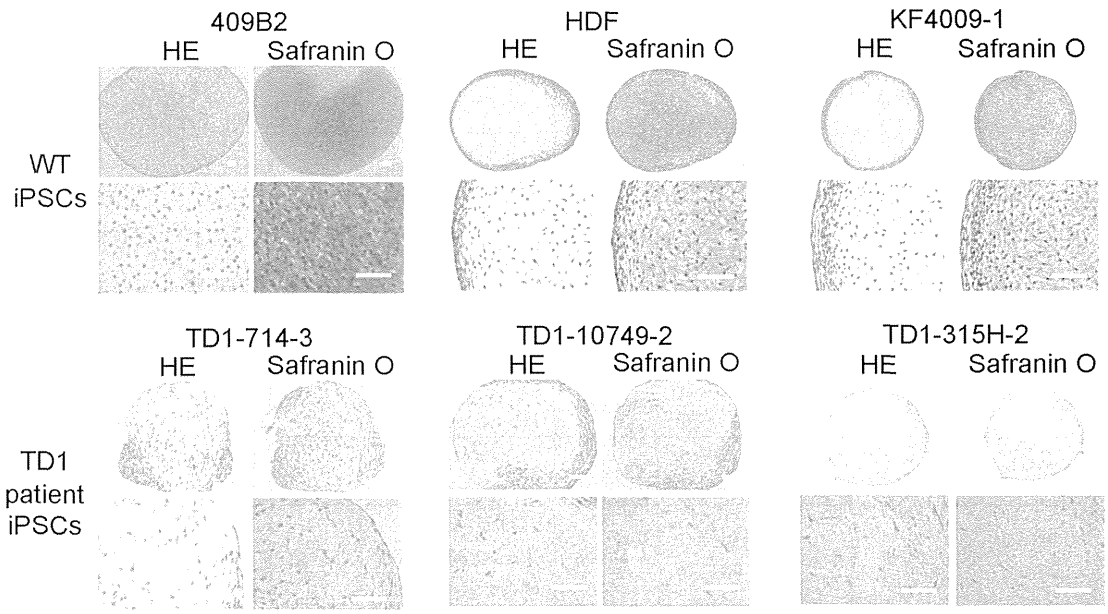

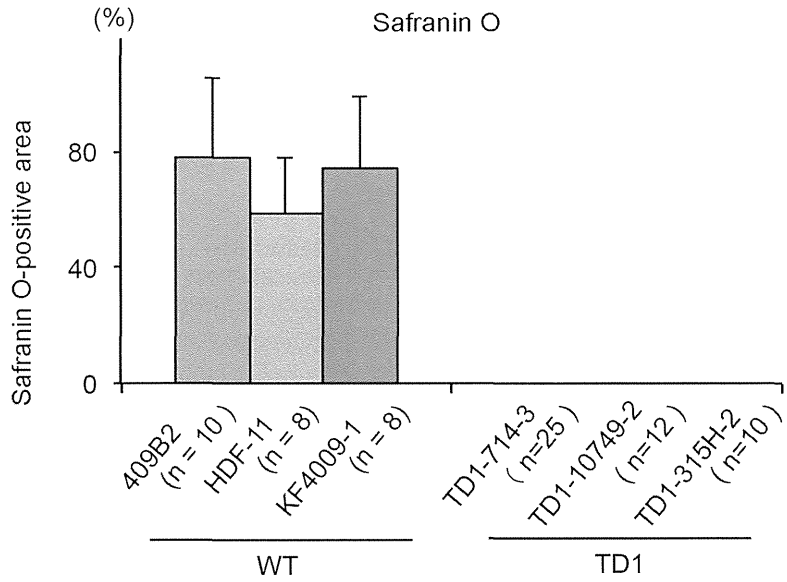

Extended Data Figure 2 | The results of a histological analysis of particles formed by chondrogenically differentiated wild-type and TD1 iPSCs on day 42. The data were collected from three independent wild-type and three independent TD1 iPSC lines which were derived from three individuals, respectively. Top: three iPSC lines established from different control individuals all formed cartilaginous particles (top panels), whereas three iPSC lines established from different patients formed particles which lacked cartilaginous elements (bottom panels). Scale bars, 50 μm. Bottom: the area of the Safranin-O-positive region was divided by the total area of the particle. The error bars denote the means ± s.d. The number of particles examined is indicated at the bottom.

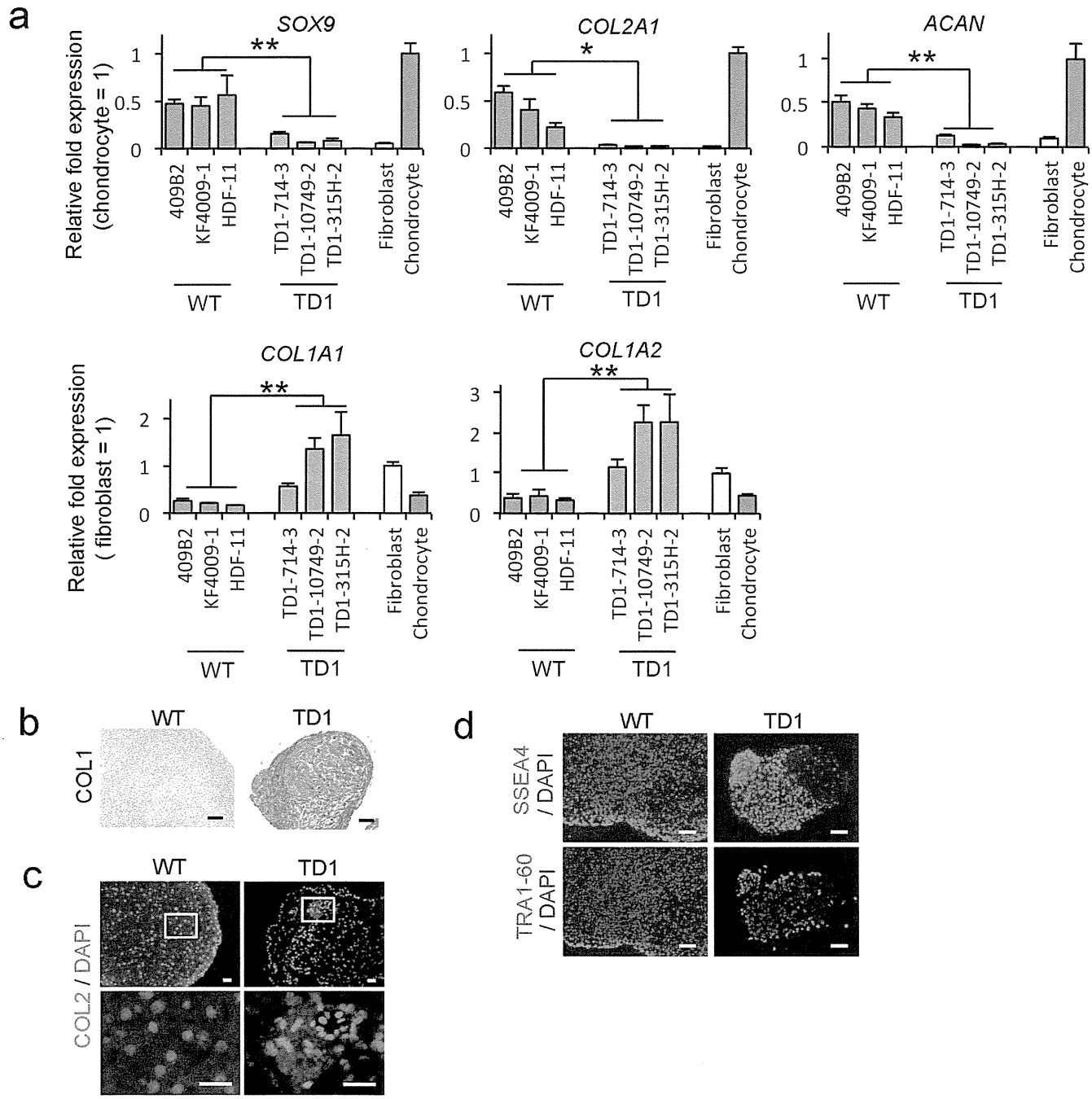

Extended Data Figure 3 | Results of the expression analysis of chondrogenically differentiated wild-type iPSCs and TD1 iPSCs. **a**, The results of a real-time RT–PCR expression analysis of marker genes in chondrogenically differentiated iPSCs lines on day 28. The data were collected from three independent wild-type and three independent TD1 iPSC lines which were derived from three individuals, respectively. Chondrocytes, re-differentiated human fetal chondrocytes; fibroblasts, dermal fibroblasts. $^{*}P < 0.05$ and $^{**}P < 0.01$ ($n = 3$ technical replicates) by the Tukey–Kramer post-hoc test. The error bars denote the means ± s.d. **b–d**, Immunohistochemical detection of the expression of type I collagen (**b**), type II collagen (**c**), SSEA4 (**d**, upper panels) and TRA1-60 (**d**, lower panels) in the particles formed by chondrogenically differentiated wild-type iPSCs (409B2) and TD1 iPSCs (TD1-714-3) on day 42. **b**, **c**, The images are representative of three independent experiments. **d**, The images are representative of experiments using three TD1-iPS clones established from three different patients. Scale bars, 50 μm (**b**, **d**); 25 μm (**c**).

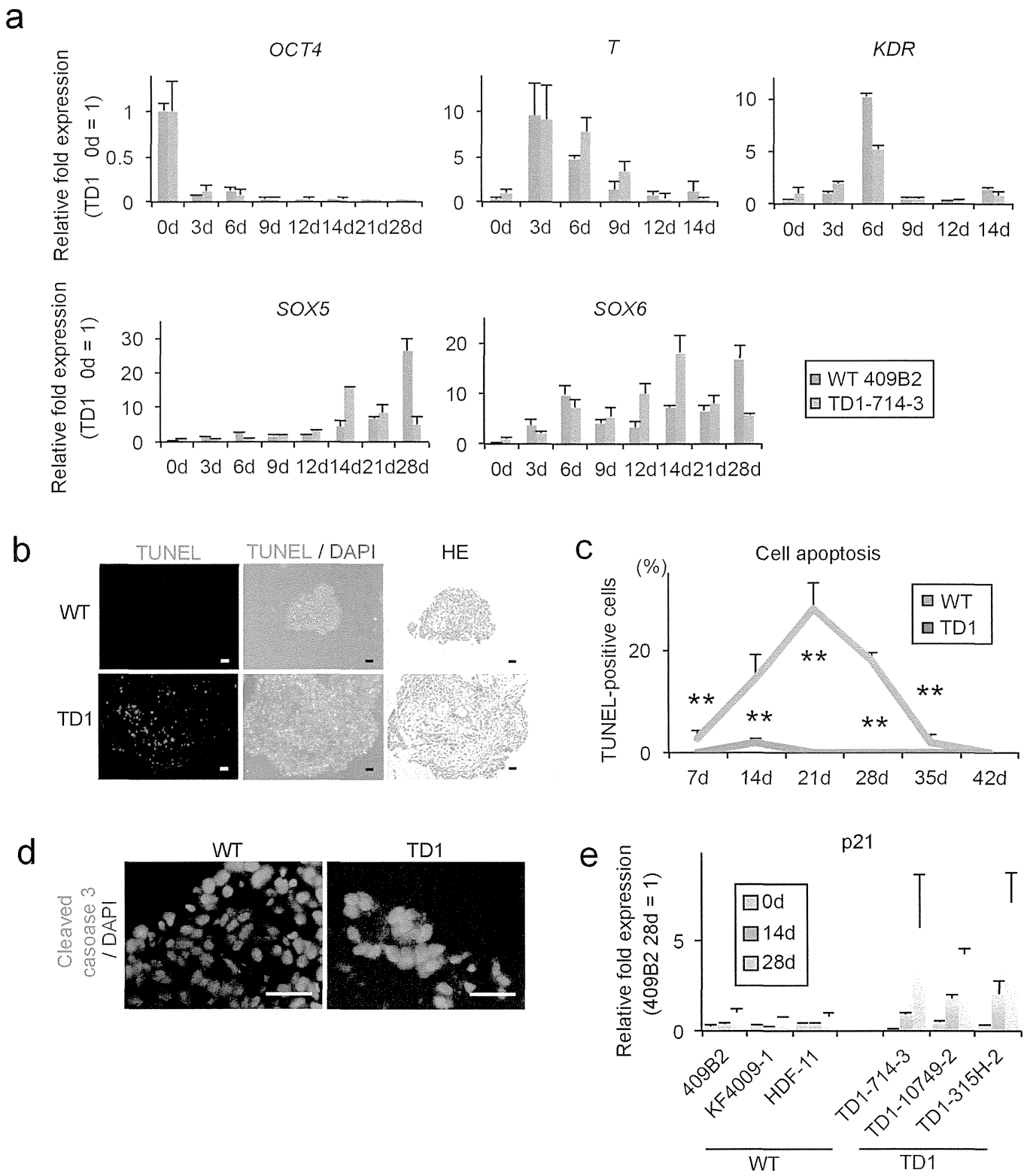

Extended Data Figure 4 | Expression levels of markers and apoptosis in chondrogenically differentiated wild-type and TD1 iPSCs. a, Time course of the changes in the expression of markers in iPSCs subjected to chondrogenic differentiation, as determined by real-time RT–PCR ($n = 3$ technical replicates). **b**, The results of the TUNEL assay of particles formed by chondrogenically differentiated iPSCs (409B2 and TD1-714-3) on day 21. Scale bars, 50 μm. The images are representative of two independent experiments. **c**, The ratio of the numbers of TUNEL-positive cells per the total cell number during the chondrogenic differentiation of wild-type iPSCs (409B2) and TD1 iPSCs (TD1-714-3). $^{**}P < 0.01$ for TD1-iPSC-derived cells compared to wild-type iPSC-derived cells on each day after chondrogenic differentiation ($n = 3$ particles), *t*-test. **d**, Immunohistochemical findings of the expression of cleaved-caspase 3 in the particles formed by chondrogenically differentiated wild-type iPSCs (409B2) and TD1 iPSCs (TD1-714-3) on day 28. Scale bars: 25 μm. The images are representative of two independent experiments. **e**, The results of a real-time RT–PCR expression analysis of p21 in chondrogenically differentiated TD1 iPSCs on days 0, 14 and 28 ($n = 3$ technical replicates). The data were collected from three independent wild-type and three independent TD1 iPSC lines which were respectively derived from three individuals. The error bars denote the means ± s.d.

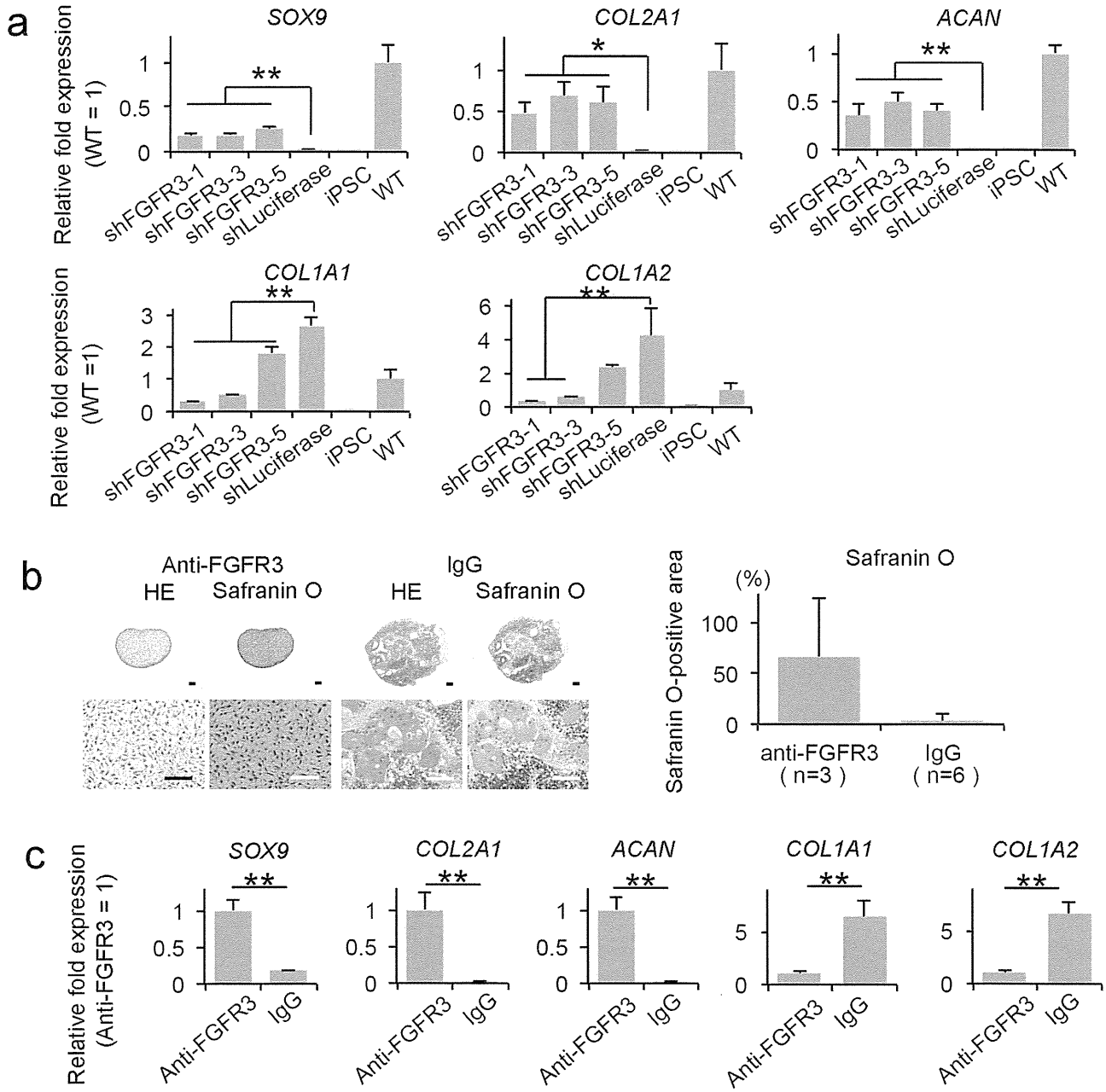

Extended Data Figure 5 | Rescuing the chondrogenically differentiated TD1 iPSCs (TD1-714-3) by *FGFR3* knockdown and treatment with a FGFR3 neutralizing antibody. a, Results of a real-time RT–PCR expression analysis of marker genes on day 28. iPSC, undifferentiated TD1 iPSCs; WT, chondrogenically differentiated wild-type iPSCs (409B2) on day 28. $*P < 0.05$; $**P < 0.01$, Tukey–Kramer post-hoc test ($n = 3$ technical replicates). The data were collected from three independent clones respectively bearing three different *FGFR3* shRNAs. **b**, A FGFR3 neutralizing antibody was added to the medium during the chondrogenic differentiation of TD1 iPSCs to induce the formation of cartilaginous particles. IgG was added as a control. The results of a histological analysis of the particles. Left: histological sections of particles were stained with haematoxylin and eosin or Safranin O. Scale bars, 50 μm. Right: the area of the Safranin-O-positive region was divided by the total area of the particle. The number of particles examined is indicated at the bottom. **c**, The results of a real-time RT–PCR expression analysis of marker genes in chondrogenically differentiated TD1 iPSCs treated with the FGFR3 neutralizing antibody on day 28. $*P < 0.05$; $**P < 0.01$ by the *t*-test ($n = 3$ technical replicates). Error bars denote the means ± s.d.

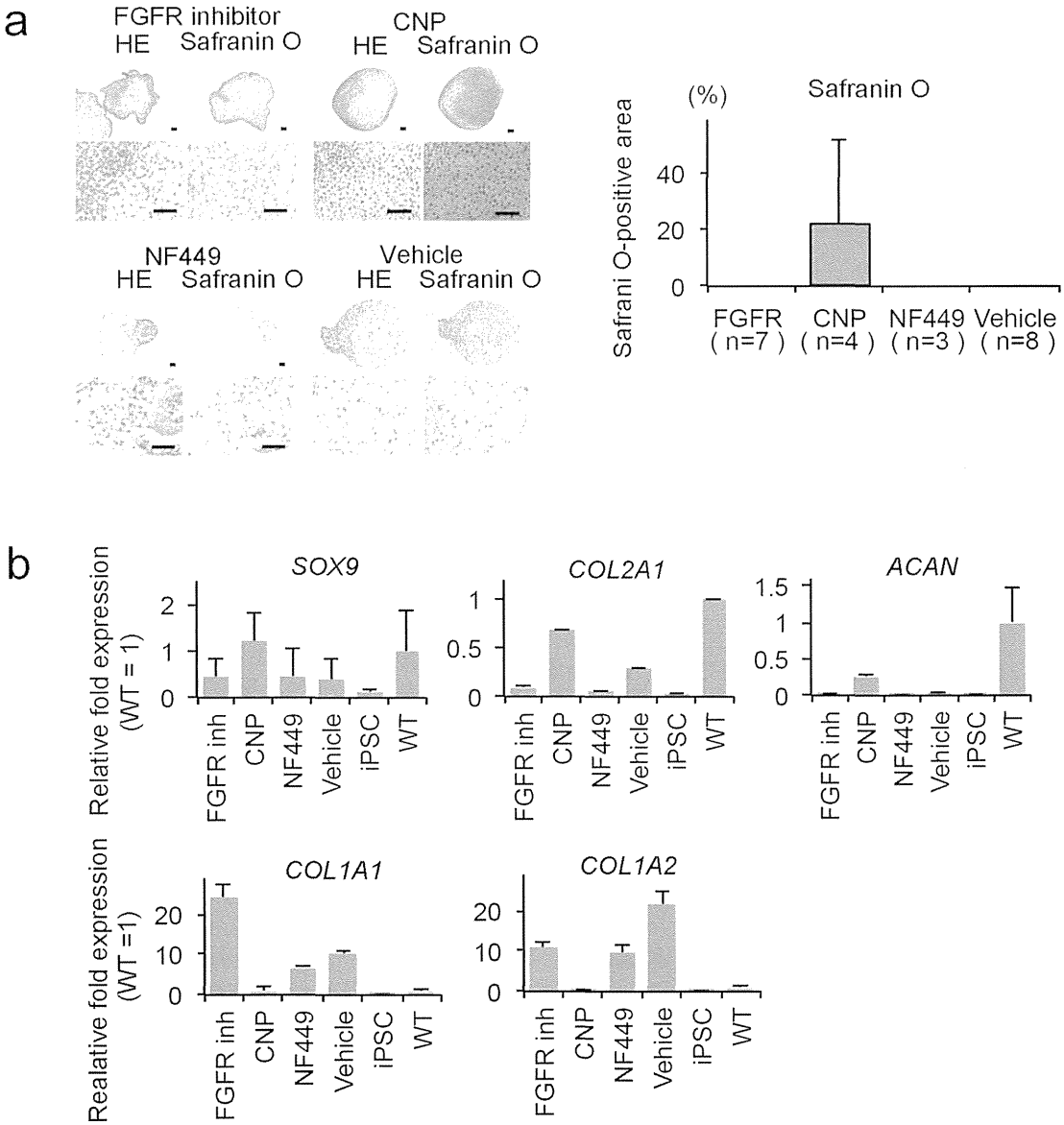

Extended Data Figure 6 | Screening for molecules that rescue chondrogenically differentiated TD1 iPSCs (TD1-714-3). **a**, Candidate molecules or vehicle were added to the medium during the chondrogenic differentiation of TD1 iPSCs. The histology of the particles was examined on day 42. Left: histological sections of particles were stained with haematoxylin and eosin or Safranin O. The addition of a FGFR inhibitor and a G-protein antagonist, NF449, failed to recover the cartilage formation of chondrogenically differentiated TD1 iPSCs under the conditions examined. The FGFR inhibitor used in this experiment inhibits not only FGFR3 but also FGFR1 and FGFR2, which might have adversely affected the cartilage formation. The addition of CNP led to the partial recovery of cartilage formation. Scale bars, 50 μm. Right: the area of the Safranin O-positive region was divided by the total area of the particle. The number of particles examined is indicated at the bottom. The data are representative of two independent experiments. **b**, The results of a real-time RT–PCR expression analysis of marker genes in chondrogenically differentiated TD1 iPSCs treated with various factors on day 28. The addition of CNP increased the expression of chondrocyte marker genes and decreased the expression of fibroblast marker genes in the chondrogenically differentiated TD1 iPSCs. iPSC, undifferentiated TD1 iPSCs; WT, chondrogenically differentiated wild-type iPSCs (409B2) on day 28. The final concentrations of each molecule were: FGF inhibitor, 1 μM; NF449, 25 μM; and CNP, 100 nM ($n = 3$ technical replicates). Error bars denote the means ± s.d.

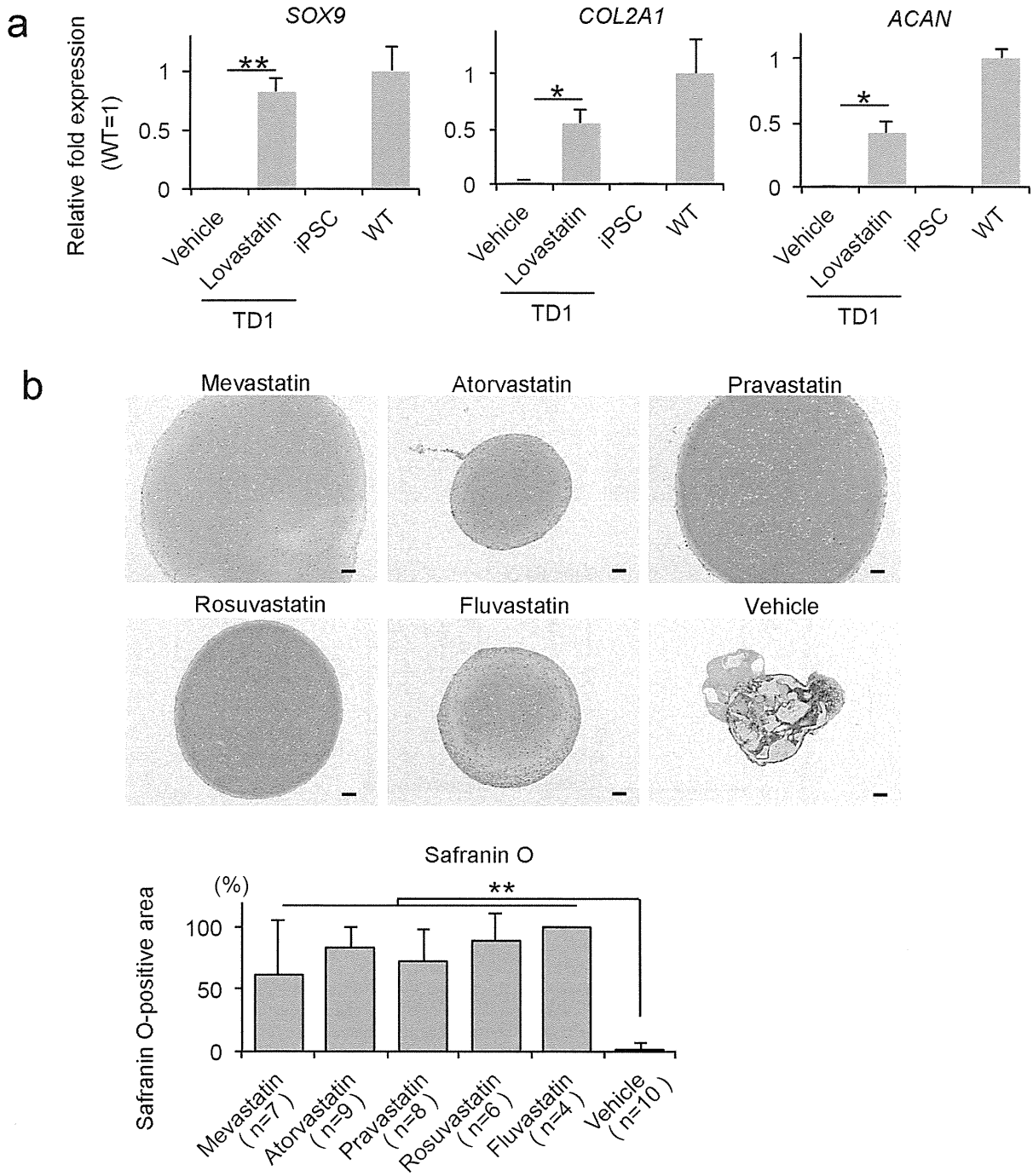

Extended Data Figure 7 | Effects of statins on chondrogenically differentiated TD1 iPSCs. **a**, The results of a real-time RT–PCR expression analysis of marker genes on day 28. TD1 (TD1-714-3) and wild-type (409B2) iPSCs were chondrogenically differentiated in the presence or absence of lovastatin (1 μM). TD1, chondrogenically differentiated TD1 iPSCs; iPSC, undifferentiated TD1 iPSCs; WT, chondrogenically differentiated wild-type iPSCs ($n = 3$ technical replicates). The data are representative of two independent experiments. **b**, Rescue of chondrogenically differentiated TD1 iPSCs by statin treatment. Mevastatin, atorvastatin, pravastatin, rosuvastatin or fluvastatin (each 1 μM) was added to the medium during the chondrogenic differentiation of TD1 iPSCs. On day 42, the particles were subjected to a histological analysis. Top: histological sections of particles were stained with haematoxylin and eosin or Safranin O. Scale bars, 50 μm. Bottom: the area of the Safranin-O-positive region was divided by the total area of the particle. The number of particles examined is indicated at the bottom. The data are representative of three independent experiments. The error bars denote the means ± s.d. $^{*}P < 0.05$; $^{**}P < 0.01$ by the Tukey–Kramer post-hoc test.

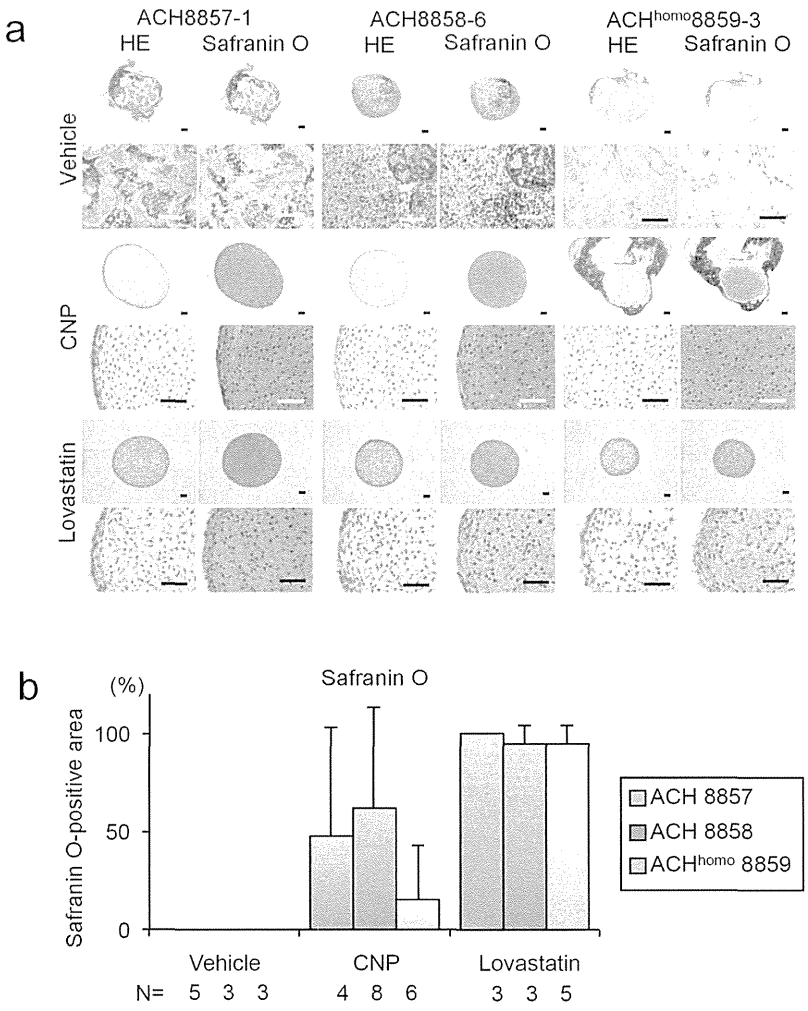

Extended Data Figure 8 | Rescue of chondrogenically differentiated ACH iPSCs by statin treatment. HDFs were obtained from two ACH patients (ACH-8857 and ACH-8858) bearing a heterozygous G380R mutation in the *FGFR3* gene (Extended Data Fig. 1a). HDFs were also obtained from an individual (ACHhomo-8859) whose parents both had ACH, who showed a more severe phenotype of chondrodysplasia than typical ACH, and who was homozygous for the G380R mutation in the *FGFR3* gene. We generated more than three iPSC lines for each patient and analysed one iPSC line (ACH-8857-1, ACH-8858-6 and ACHhomo-8859-3) derived from each patient's HDFs. We confirmed that all iPSC lines expressed SSEA4 and TRA1-60, and formed teratomas containing all three germ layers in mice. Lovastatin and CNP were added to the medium during the chondrogenic differentiation of ACH iPSCs. The histology of particles was examined on day 42. **a**, Histological sections of particles were stained with haematoxylin and eosin or Safranin O. Scale bars, 50 μm. **b**, The area of the Safranin-O-positive region was divided by the total area of the particle. The number of particles examined is indicated at the bottom. The error bars denote the means ± s.d.

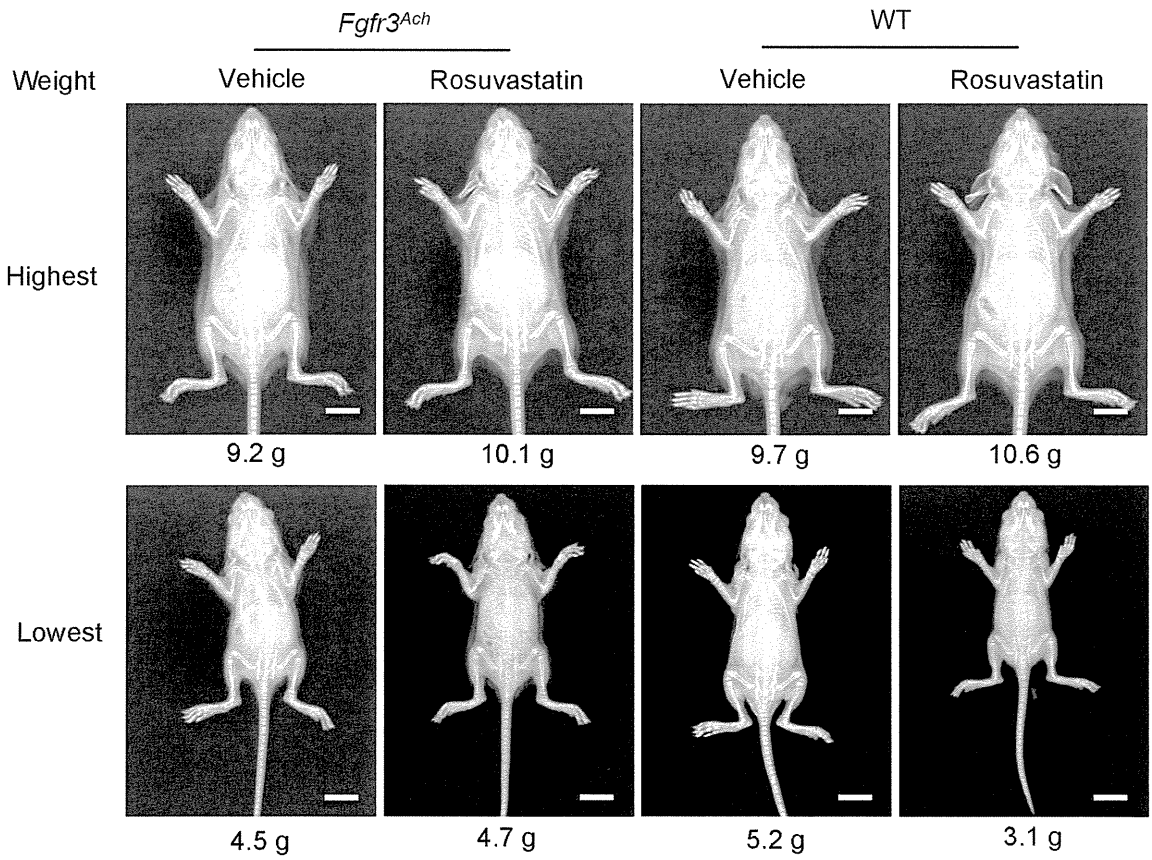

Extended Data Figure 9 | X-ray images of *Fgfr3*^{Ach} and wild-type mice treated with rosuvastatin or vehicle. The images of the mice with lowest and highest weights in each group are shown. The weight (g) of each mouse is indicated at the bottom of each panel. Scale bars, 10 mm.

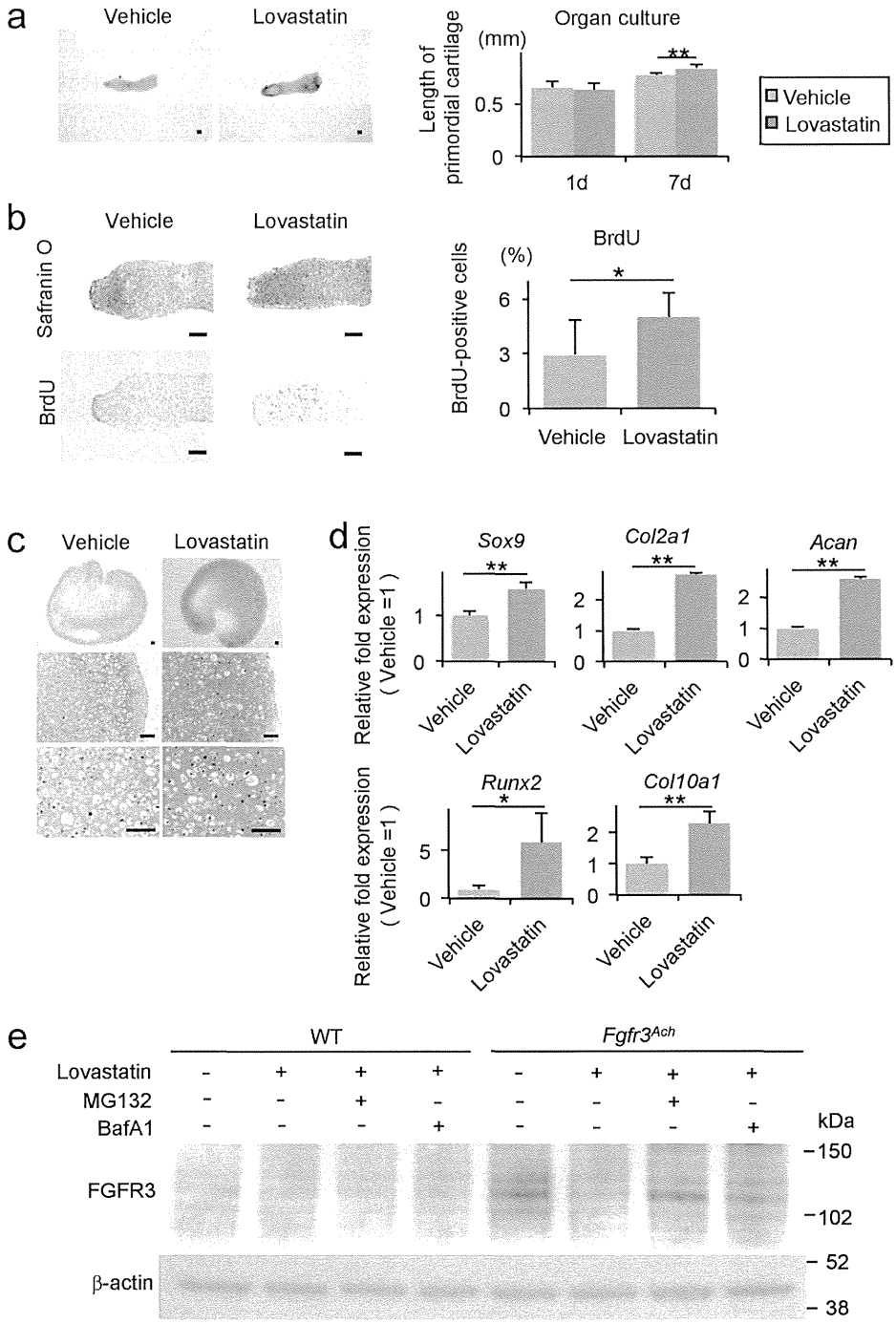

Extended Data Figure 10 | Organ culture of metatarsal primordial cartilage (a, b), pellet culture of primary chondrocytes (c, d) and culture of primary chondrocytes (e) from *Fgfr3*^{Ach} mice in the presence or absence of lovastatin. **a**, Left: images of cartilage on day 7. Right: mean lengths of the cartilage on day 1 and day 7 ($n = 8$ cartilage samples). **b**, Cartilage on day 7 was treated with BrdU. Left: histological sections were stained with Safranin O and immunostained with BrdU. Right; number of BrdU-positive cells were divided by the total number of cells ($n = 7$ cartilage samples). **c**, Histological sections of pellets cultured for 14 days. The images are representative of three pellets. **d**, The results of the real-time RT–PCR expression analysis of pellets cultured for 14 days (*Sox9*, *Col2a1* and *Acan*) and 28 days (*Runx2* and *Col10a1*) ($n = 3$ technical replicates). The data are representative of two independent experiments. **e**, Primary chondrocytes from wild-type and *Fgfr3*^{Ach} mice were cultured in the presence or absence of lovastatin, MG132 or bafilomycin A1, and were subjected to an immunoblot analysis using an anti-FGFR3 antibody. The images are representative of two independent experiments. Error bars denote the means ± s.d. $*P < 0.5$; $**P < 0.01$ by the *t*-test. Scale bars, 50 μm.